Submarine Landforms and Glacimarine Sedimentary Processes in Lomfjorden, East Spitsbergen

Katharina Streuff[a,*], Colm Ó Cofaigh[a], Riko Noormets[b], Jeremy Lloyd[a]

[a] *Durham University, Department of Geography, South Road, Durham DH1 3LE, United Kingdom*
[b] *The University Centre in Svalbard (UNIS), P.O. Box 156, N-9171 Longyearbyen, Norway*

Abstract

Understanding the role of fjords in modulating the long-term interaction between ice sheets and glaciers with the surrounding ocean requires the investigation of glacigenic landform and sediment archives. In Svalbard, there is a wealth of data from fjords in west Spitsbergen that constrains the glacial history of this sector of the Svalbard-Barents Sea Ice Sheet (SBIS) since the Last Glacial Maximum (LGM), and the nature and timing of subsequent ice retreat. In contrast, however, very little is known about the glacial history of fjords in east Spitsbergen.

This paper combines multibeam swath-bathymetry, sub-bottom profiles, lithological data and radiocarbon dates from Lomfjorden, Svalbard, to provide the first insights into the dynamics of tidewater glaciers and associated glacimarine sedimentary processes in a northeast Spitsbergen fjord. At the LGM, a fast-flowing ice stream drained the SBIS through Lomfjorden, serving as a tributary to a south-north flowing ice stream in Hinlopenstretet. Ice advance is recorded by streamlined bedrock, glacial lineations and drumlins. A radiocarbon date of ∼9.7 ka BP from the outer fjord provides a minimum date for retreat of this

*Corresponding author
Email addresses: katharina.streuff@durham.ac.uk (Katharina Streuff), colm.ocofaigh@durham.ac.uk (Colm Ó Cofaigh), riko.noormets@unis.no (Riko Noormets), j.m.lloyd@durham.ac.uk (Jeremy Lloyd)

ice stream, and suggests that Lomfjorden was ice-free earlier than fjords in west Spitsbergen. Ice retreat occurred in a slow and step-wise manner, indicated by the presence of recessional moraines and De Geer moraines. By 4.5 ka BP the local tidewater glaciers had probably retreated inland of their present positions. The limited extent of glacigenic landform assemblages in front of these glaciers implies that any Holocene re-advances were probably restricted.

The principal sedimentary processes during deglaciation were suspension settling from meltwater, causing deposition of weakly stratified, bioturbated mud in ice-distal settings at rates of 0.02–0.08 cm a^{-1}, and gravitational mass flows forming sandy turbidites in ice-proximal areas. Iceberg ploughmarks and ice-rafted debris provide evidence for the presence of large icebergs during deglaciation.

Our data suggest an early and extensive deglaciation in east Spitsbergen fjords and show that previous reconstructions of the extent of the SBIS need to be revised as new data emerges from east Spitsbergen. The data confirm that tidewater glaciers from different regions of Spitsbergen behaved differently since the LGM, and that large variations in landform-sediment assemblages occur even within geographically adjacent fjords.

Keywords: Fjords, glacimarine sediments, submarine landforms, east Spitsbergen, Holocene, ice retreat

---

1. Introduction

The landforms and sediments deposited beneath and in front of modern glaciers are an important archive of past glacial dynamics and of glacier response to climatic forcing (e.g. Cottier et al., 2010; Forwick et al., 2010), but glacier beds and submarine forelands are often relatively inaccessible due to the presence of

overlying glacier ice or sea ice in fjords. In this context Svalbard is of particular interest, as the ongoing retreat of many fjord-terminating tidewater glaciers has recently exposed well-preserved glacial and glacimarine landform-sediment assemblages (e.g. Plassen et al., 2004; Ottesen & Dowdeswell, 2006; Ottesen et al., 2008; Forwick et al., 2010; Kempf et al., 2013; Flink et al., 2015; Streuff et al., 2015). Furthermore, fjords in Spitsbergen, the largest island of the archipelago, are usually ice-free during summer and thus enable the acquisition of high-resolution seismic data and sediment cores. These data provide valuable insights into the nature of the glacial deposits, and thus, by inference, into the associated glacigenic processes (e.g. Syvitski, 1989; Sexton et al., 1992; Boulton et al., 1996; Cai et al., 1997; Forwick et al., 2010). Fjords along the west coast of Spitsbergen have received increasing attention during the last two decades and resulting studies have documented characteristic landform assemblages in front of many tidewater glaciers. These include (overridden) recessional moraines, glacial lineations, eskers, terminal moraines, debris flow lobes, in some cases crevasse-squeeze ridges, and annual push moraines (e.g. Ottesen & Dowdeswell, 2006; Ottesen et al., 2008). Terminal moraines in the fjords commonly mark the extent of glacier advances during the Holocene, which occurred either due to climatic cooling, particularly during the Little Ice Age (LIA), or as a consequence of glacier surges (e.g. Plassen et al., 2004; Ottesen & Dowdeswell, 2006; Ottesen et al., 2008; Forwick & Vorren, 2011; Flink et al., 2015; Streuff et al., 2015; Burton et al., 2016). Conversely, very little is known about the fjords along Spitsbergen's eastern coast, where, to our knowledge, only Hambergbukta in the south has been studied in detail (Noormets et al., 2016a,b). Hence, our limited understanding of oceanography, glaciology, glacigenic landform assemblages and sedimentary processes in east Spitsbergen fjords inhibits the development of accurate ice sheet models, which are crucial to understanding the complex

climatic system and the role of its individual components on ice sheet dynamics and deglaciation history in Svalbard and the Barents Sea (Patton et al., 2015; Stokes et al., 2015; Gowan et al., 2016; Kirchner et al., 2016).

This study is the first to address in detail the glacimarine environment, including oceanography and sedimentary processes, as well as landforms in a northeast Spitsbergen fjord, and the first to provide constraints on the timing of ice retreat in this area. We present and analyse multibeam swath-bathymetric and sub-bottom profiler data, sediment cores, CTD data and a suite of radiocarbon dates from Lomfjorden, northeast Spitsbergen, from which we reconstruct the Holocene dynamics of the local tidewater glaciers and evaluate whether glaciers in east Spitsbergen behaved differently to those in the west.

2. Study Area and Background

2.1. Physiographic Setting

Lomfjorden is located in northeastern Spitsbergen between ~79°21'N, 17°40'E and 79°43'N, 18°20'E. It is orientated south to north, opens into Hinlopenstretet, a strait between Spitsbergen and Nordaustlandet, and is located in a relatively protected environment (Fig. 1). Lomfjorden is 35 km long, 2–10 km wide and up to 200 m deep. A major fault zone, the Lomfjorden-Agardhbukta Fault Zone (LAFZ), runs through the centre of the fjord, with Palaeozoic and Mesozoic sediments defining Lomfjorden's eastern coast, and Neoproterozoic basement rocks defining the west (Dallmann et al., 2002). There are three tidewater glaciers along Lomfjorden's shore, Glintbreen and Kantbreen in the east, and Valhallfonna in the northwest (Fig. 1). At the head of Lomfjorden, the Veteranen glacier previously reached tidewater but has now retreated onto land where it formed numerous moraines (Fig. 1). Other currently terrestrial

glaciers are Odinjøkulen and Frøyabreen along the eastern shore and Bivrostfonna, Frostbreen, Skinfaksebreen and Gullfaksebreen along the western shore (Fig. 1). Two small embayments are located along the fjord's western shore, Faksevågen in the south and De Geerbukta in the north, which host Skinfaksebreen and Gullfaksebreen, respectively (Fig. 1). The catchment areas of the tidewater glaciers are mainly underlain by carbonate bedrock (dolomites and limestones) with lesser quartzites and metagreywacke (Dallmann et al., 2002).

2.2. Glacial Background

Contrary to the well-investigated history of the Svalbard-Barents Sea Ice Sheet in west Spitsbergen and north and east of Svalbard (e.g. Mangerud et al., 1992; Elverhøi et al., 1995; Landvik et al., 1995, 1998; Ottesen et al., 2005; Ingólfsson & Landvik, 2013), very little is known about the glaciological evolution of fjords in east Spitsbergen, including Lomfjorden. Oceanographic investigations document that the waters on the eastern side of Svalbard are mostly fed by relatively cold and fresh Arctic Water and that the inflow of warm and saline Atlantic water, so common on west Spitsbergen, is absent in the east (cf. e.g. Svendsen et al., 2002; Hald et al., 2004; Ślubowska-Woldengen et al., 2007). Nevertheless, inflow of warmer Atlantic water into Hinlopenstretet was indicated by lithological records from the northern Svalbard margin (e.g. Koç et al., 2002; Ślubowska et al., 2005). Only recently have summer sea ice conditions allowed the acquisition of geophysical and lithological data in eastern Svalbard and thus enabled the reconstruction of the glacial history around Kong Karls Land and Edgeøya (Dowdeswell et al., 2010; Hogan et al., 2010). General consensus is that large parts of the Barents Sea and all of Svalbard were glaciated during the Last Glacial Maximum (LGM), ∼20 ka BP, when the large fjord systems on Svalbard channelled fast-flowing ice streams that extended to the continental

shelf edge (e.g. Elverhøi et al., 1993; Landvik et al., 1998; Svendsen et al., 2004; Ottesen et al., 2005; Ingólfsson & Landvik, 2013). During this time ice flowed eastwards through Olgastretet and Erik Eriksenstretet, westwards towards Isfjorden, and northwestwards through Hinlopenstretet and Wijdefjorden from a large ice dome located just west of Kong Karls Land at the southern entrance of Hinlopenstretet (Fig. 1a; Landvik et al., 1998; Dowdeswell et al., 2010; Hogan et al., 2010). The timing of the onset of deglaciation in this part of the Barents Sea is still debated, with ages ranging from 15 ka BP to 13.4 ka BP (Jones & Keigwin, 1988; Elverhøi et al., 1995; Kleiber et al., 2000). During deglaciation ice retreated relatively slowly and in a step-wise manner, depositing recessional moraines in Erik Eriksen Strait (Dowdeswell et al., 2010; Hogan et al., 2010). Edgeøya and Barentsøya southeast of Spitsbergen became ice-free around 10.3 ka BP, when a major calving event resulted in the disintegration of the marine-based sector of the Svalbard-Barents Sea Ice Sheet (Landvik et al., 1995).

3. Material and Methods

Swath bathymetry, subbottom profiler (chirp) data, and seven sediment cores provide the basis for this study. Bathymetric data were collected by the Norwegian Hydrographic Survey in July and August 2011, using a Kongsberg Simrad Multibeam EM3002 on the vessel *Hydrograf*. The data were processed in DMagic, gridded to a resolution of 5 m and visualised and interpreted in the Fledermaus v7 Software. Chirp data were acquired by the University Centre in Svalbard on *R/V Helmer Hanssen* in September 2014, using an EdgeTech 3300-HM subbottom profiler operating at a pulse mode of 2-16 kHz bandwidth and 3 ms pulse length. The data were processed using the EdgeTech Software and visualised in IHS The Kingdom Software. Seven gravity cores were taken during the same cruise and provide the basis for the lithology section (Table 1).

At two of the core sites and one additional site conductivity-temperature-depth (CTD) information was obtained from the water column (Table 1). Gravity cores were retrieved with a 1900 kg heavy gravity corer with a 6 m long steel barrel. Upon retrieval the cores were cut into sections of up to 110 cm long and run through a loop sensor to measure the magnetic susceptibility of the sediments. The cores were then split into working and archive halves. For the water content 1 cm-thick sediment slabs were taken in 8-cm intervals, weighed, dried at 60°C and weighed again. The samples were subsequently wet-sieved through mesh sizes of 500, 250, 125 and 63 μm to determine the grain size distribution within the cores. Core logs were generated based on the visual description of the sediment surface aboard the ship and at the University Centre in Svalbard. The archive halves (in some cases the working halves) were subsequently x-rayed using a GEOTEK Thermo Kevex PSX10-65W-Varian2520DX with a voltage of $\sim$95 kV and a current of around 150 μA. Correlation between seismo- and lithostratigraphy and calculation of acoustic facies thickness was done by converting sediment core depth from m to ms, and facies thickness from ms to m, assuming an average p-wave velocity of 1500 m s^{-1} (two-way travel time). Conversions are estimates only and may lead to slight inaccuracies concerning core penetration depth and actual facies thickness. Foraminifera and, where present, bivalves, were collected from strategic locations in two of the gravity cores, GC12 in the outer fjord and GC08 in the inner fjord, and were submitted to Beta Analytic for Accelerator Mass Spectrometry radiocarbon dating. The obtained conventional ^{14}C ages were calibrated using the MARINE13 calibration with a marine reservoir effect of 400 years and a Delta R of 100 $\pm$ 39 years (Table 2; cf. Long et al., 2012).

Table 1: Gravity cores and CTD data used in this study.

Sample ID	CTD	Recovery [cm]	Water depth [m]	Latitude (N)	Longitude (E)
GC05 + CTD	St611	263	68	79°23.033'	17°43.325'
GC06		88.5	75	79°23.488'	17°45.283'
GC07		294	70	79°23.265'	17°44.163'
GC08		276	116	79°25.037'	17°51.073'
GC09 + CTD	St612	305	119	79°25.773'	17°52.310'
GC10		105	118	79°33.702'	17°47.905'
GC12		339	200	79°36.392'	17°57.003'
CTD	St613		205	79°37.571'	18°04.736'

4. Results

4.1. Seafloor Morphology

Based on the available swath-bathymetric data, we define (1) streamlined bedrock highs, (2) glacial lineations, (3) drumlins, (4) recessional moraines and in some cases associated debris lobes, (5) De Geer moraines, (6) submarine channels and mass-transport deposits, and (7) iceberg ploughmarks in Lomfjorden. Their distribution in the fjord is shown in Figure 2.

4.1.1. Large Longitudinal Ridges – Bedrock

Four large, straight to slightly sinuous ridges, R1, R2, R3, and R4 occur in inner and central Lomfjorden (Fig. 2). They are orientated NNW–SSE, obliquely to the main fjord axis, and are composed of several segments, which are 60–100 m high, up to 1.2 km wide and 150–2500 m long. These segments generally have sharply defined crests which are composed of multiple peaks (Fig. 3b). The ridges occur in water depths between 20 and 120 m and reach overall lengths between 2 and 5.5 km. They appear streamlined in the inner fjord, where they are also overprinted by drumlins (see Figs. 2, 3 and section 4.1.3 below). R4 is the submarine extension of the island Footøya (Fig. 2) and its most distal segment has three crests along its main axis. In addition to the ridges in the central and inner fjord, several large bathymetric highs occur in the outer fjord (Fig. 2). These are around 60 m high and 0.5–3 km wide.

The irregular and discontinuous character of the ridge crests as well as their large scale is unlike any glacially-derived submarine ridges in Spitsbergen (cf. e.g. Solheim & Pfirman, 1985; Boulton et al., 1996; Ottesen et al., 2008). Furthermore, we would expect pro- or subglacial ridges to be formed either perpendicular or (sub-)parallel to the direction of ice flow. The ridges' oblique orientation, their morphology, and their location in the fjord is therefore at odds with a solely glacial origin and we suggest that the ridges and, in the outer fjord, the bathymetric highs, are composed of bedrock that has been partially streamlined. This is based on the following: (1) the ridges' orientation is similar to some of the faults in the area (Figs. 1, 2), (2) R4 is the submarine extension of the island Footøya (Fig. 2), and (3) the ridges are similar to bedrock ridges in Van Keulenfjorden (Kempf et al., 2013).

Two small longitudinal, streamlined ridges (ra and rb) follow the bathymetric contours of R1-R4 (Figs. 2, 3b). They are morphologically similar to the bedrock ridges, as ra and rb are also composed of several segments, which have straight to slightly sinuous crests with multiple peaks. However, their segments are much longer (up to 3.5 km) and lower (2–15 m high) than those of R1–R4, and are up to 150 m wide (Fig. 3b). In a few places ra and rb are overprinted by, or confluent with, the small transverse ridges described in section 4.1.4 below.

Based on similarities in morphology and orientation, these ridges could represent the small-scale equivalent of the bedrock ridges R1–R4. However, ra and rb are also, at least partially, of glacial origin, as they are streamlined and similar to the glacial lineations and drumlins observed in the fjord (see sections 4.1.2 and 4.1.3 below).

4.1.2. Elongate, Streamlined Grooves and Ridges – Glacial Lineations

Elongate grooves and ridges in the outer fjord are 2–10 m high, 700–3000 m long, up to 200 m wide and spaced at distances of between 200 and 400 m

(Figs. 2, 3d, e). Their elongation ratios, in most cases, exceed 10:1. Their crests are straight to slightly curved and are mostly round and symmetrical in cross-section (Fig. 3).

The elongate features in outer Lomfjorden appear similar to groove-ridge features described from other Spitsbergen fjords, and are thus interpreted as (mega-scale) glacial lineations (cf. Ottesen & Dowdeswell, 2006; Ottesen et al., 2008). Glacial lineations, especially those with length:width ratios exceeding 10:1 are exclusively associated with fast ice flow (Stokes & Clark, 2002; King et al., 2009). They are formed beneath a (surging) glacier or ice stream, where the soft subglacial sediments are deformed into ridges and grooves by a combination of erosion and re-deposition (Smith, 1997; Tulaczyk et al., 2001; Clark et al., 2003; Ó Cofaigh et al., 2005).

Segments of similar streamlined grooves and ridges occur around the three bedrock ridges R2–R4 in the central part of Lomfjorden (Fig. 2). They are up to 700 m long, 100 m wide, and ∼5 m high, with maximum elongation ratios of 7:1. The grooves and ridges are orientated (sub-)parallel to each other and spaced at variable distances between 50 and 100 m. They follow the contours of the bedrock ridges (Figs. 2, 3) and have thus slightly variable orientations.

These groove-ridge segments are similar to the glacial lineations in the outer fjord and were presumably formed by the same processes, i.e. sediment deformation beneath the glacier. Nevertheless, the discontinuous character and the much smaller elongation ratios of the streamlined segments indicate that the conditions during their formation may have been different. Possible explanations for the short lengths could be (1) insufficient sediment, (2) a less deformable glacier bed, and/or (3) slower ice flow. The outcropping bedrock highs at the seafloor may, for example, have acted as "sticky spots" or obstacles and thus slowed glacier flow.

4.1.3. Small, Streamlined Ridges – Drumlins

Small, elongate (sub-)parallel ridges occur in close proximity to the bedrock ridges in central Lomfjorden (Fig. 2), and are between 250 and 1500 m long, up to 200 m wide, and ∼10 m high. They have straight, sharply defined crests and are spaced at distances between 50 and 200 m (Fig. 3b, f–h). The ridges are orientated in the direction of the main fjord axis and appear slightly broader and blunter at their ice-proximal (stoss) sides, where they often have a small bulge (Fig. 3h). Their distal ends appear tapered and terminate in a point.

Although some of the small ridges in central Lomfjorden appear similar to glacial lineations from other Spitsbergen fjords (Flink et al., 2015; Streuff et al., 2015), the blunt stoss sides, tapered lee ends, dimensions and 'tear-drop' shape in planform are more consistent with these features being drumlins (cf. Clark et al., 2009; Spagnolo et al., 2010).

4.1.4. Transverse Ridges – Recessional Moraines

Small ridges in front of Valhallfonna in the outer fjord (Fig. 2) are parallel to the ice margin and to each other, are continuous, and up to 3 km long (Fig. 4a–c). They are orientated transverse to the inferred direction of ice flow, are 2–5 m high, around 30 m wide and occur in water depths of around 10 m (Fig. 4a, b). The ridges are generally symmetrical in cross-section and have well-defined, sharp, and slightly sinuous crests. Several of these ridges are observed to merge in places and exhibit branching. They are spaced at distances of approximately 50, 100, or 150 m. The outermost ridge furthest away from the current ice margin is slightly larger and is up to 20 m high, 3.6 km long, and ∼400 m wide (Fig. 4a, b).

In front of Glintbreen/Kantbreen in inner Lomfjorden, two of these ridges are ∼1 km long and occur spaced at ∼50 m in a water depth of around 10

m. Again, the outermost ridge is slightly higher (10 m) than the inner one (5 m). In front of both Valhallfonna and Glintbreen/Kantbreen lobate landforms occur on the outermost ridges' distal flank and cover areas of approximately 200 x 1500 and 250 x 850 m^2. In front of Frøyabreen in the east, four of the small ridges occur (Fig. 2) and are up to 1 km long, ∼5 m high and spaced at approximately 50 m.

Ridges in the central fjord are morphologically similar to those in front of the tidewater glaciers, but are slightly wider (∼100 m) and much shorter (∼500 m). These shorter ridges are predominantly sub-perpendicular to the main fjord axis, parallel to each other, and are, in some cases, closely associated with ridge ra described in section 4.1.1; either as perpendicular "branches" to one side of the ridge or cross-cutting the ridge at a ∼90°-angle. They are irregularly spaced, with distances of 700–2000 m between individual ridges (Figs. 3b, 4d).

In terms of dimensions, morphology and orientation, the transverse ridges in Lomfjorden are similar to annual push moraines described from other fjords in Spitsbergen (Ottesen & Dowdeswell, 2006; Ottesen et al., 2008), which suggests that the ridges in Lomfjorden were also formed as end moraines at a glacier grounding line. Annual push moraines result from small winter re-advances or still-stands of the glacier during overall retreat, and are often the result of shore-fast sea ice preventing iceberg calving and thus further retreat of the glacier margin (e.g. Boulton, 1986; Ottesen & Dowdeswell, 2006; Flink et al., 2015). The symmetrical form of the Lomfjorden ridges may reflect formation from debris meltout at the grounding line rather than actual sediment push, and we therefore favour the more general interpretation of these ridges as recessional moraines.

In front of Valhallfonna in the outer fjord, the spacing at ∼50, ∼100, or ∼150 m implies that the ridges were deposited on a somewhat regular basis,

but as the ridges are not spaced at equal distances throughout, they were either not always formed annually or retreat distances between subsequent years were variable. Based on the slightly larger dimensions of the outermost ridges in front of Valhallfonna and Glintbreen/Kantbreen, these ridges may have formed as terminal moraines during an advance of the respective glacier during the LIA (cf. Plassen et al., 2004; Ottesen & Dowdeswell, 2006; Ottesen et al., 2008). They could, however, also have formed from a slightly prolonged period of glacier still-stand. The lobate deposits on the distal flanks are interpreted as glacier outwash fans or glacigenic debris lobes, formed from continuously high sediment influx either supplied from glacial meltwater streams or extruded from beneath the glacier at its grounding line (cf. e.g. Boulton, 1986; Kristensen et al., 2009). Such debris lobes are often associated with LIA advances and may thus support an interpretation of the outermost ridges as terminal moraines (Plassen et al., 2004; Ottesen & Dowdeswell, 2006; Forwick & Vorren, 2011). This is further discussed in section 5.3 below.

The much shorter ridges in the central fjord may have formed at the grounding line of an ice stream or tidewater glacier (Veteranen) retreating through the fjord, with the larger spacing indicating faster ice flow and/or irregular intervals of deposition. The shorter lengths could be linked to (1) a narrower grounding line, and/or (2) post-depositional sediment masking of parts of the ridges. The latter is supported by the abundance of glacimarine sediments in the fjord, as shown by the subbottom profiler data (section 4.2).

4.1.5. Small and Short Ridges – De Geer Moraines

Small ridges on the western flank of the innermost fjord basin are up to 2 m high and have poorly defined, smooth and indistinct crests, which appear to be interconnected in places. The ridges are orientated obliquely to each other and, in places, form a sort of diffuse ridge network (Fig. 4d). Ridge segments are up

to 500 m long and around 100 m wide. The connection and variable orientation of the crests to each other is different to the strictly (sub-)parallel recessional moraines described above (Fig. 4d).

These small ridges are interpreted as De Geer moraines (cf. Lundqvist, 1981), which usually occur as sets of ∼3 m high, up to 30 m wide and several hundred meters long, submarine, mainly transverse, and irregularly-spaced ridges (Zilliacus, 1989; Lundqvist, 2000). The formation of De Geer moraines is attributed to either (1) pushing up of subglacial sediments at the grounding line (e.g. De Geer, 1940; Boulton, 1986; Larsen et al., 1991; Blake, 2000), a process analogous to the formation of annual push moraines, or (2) the squeezing of soft subglacial sediments into basal glacier crevasses (e.g. Hoppe, 1957; Strömberg, 1965; Zilliacus, 1989; Beaudry & Prichonnet, 1991), analogous to the formation of crevasse-squeeze ridges (e.g. Solheim & Pfirman, 1985; Boulton et al., 1996; Ottesen & Dowdeswell, 2006). Both processes are possible for the formation of the ridges in inner Lomfjorden, as their indistinct appearance is different to the well-developed, sharp-crested crevasse-squeeze ridges in other Spitsbergen fjords (Ottesen et al., 2008; Flink et al., 2015). This could be related to the presence of an undersaturated, less deformable subglacial till in Lomfjorden (cf. e.g. Lovell et al., 2015), to poorly-developed crevasses within the glacier, or to post-glacial sediment infill between individual ridges masking their true appearance. The predominantly transverse orientation of the ridges and the lack of cross-cutting relationships between individual ridges are consistent with formation of the ridges as glacier end moraines. This is further supported by the limited number of well-developed superficial crevasses on Glintbreen, Kantbreen, and Veteranen, which suggests that these glaciers are not subject to the stress regime necessary to form crevasses (cf. Van der Veen, 1999; Benn & Evans, 2010). Although no guarantee, this, in turn, implies that basal crevasses

are also relatively scarce. Notwithstanding this, the distribution of the ridges as a diffuse network of partially interconnected crests appears to be more consistent with crevasse-squeezing. We therefore suggest that the ridges formed from debris-meltout at the grounding line of a retreating ice margin with some degree of crevasse-squeezing during periods of longer still-stand (e.g. Solheim & Pfirman, 1985; Boulton et al., 1996; Ottesen & Dowdeswell, 2006; Ottesen et al., 2008).

4.1.6. Steep Elongate Channels and Lobate Deposits – Submarine Channels and Mass-Transport Deposits

Elongate U- or V-shaped channels can be found along the steep fjord walls of Lomfjorden and are orientated (sub-)perpendicular to the main fjord axis. We distinguish two kinds of channels: Type-A channels with lobate deposits at their flat ends (Figs. 2, 4g-i) and Type-B channels dissociated from such deposits (Fig. 4j, k). Type-A channels are normally ∼3 m deep, up to 1 km long and usually ∼200 m wide, with slope angles of 10–20°. Lobate-shaped deposits at their mouths are up to 700 m long, 1–3 m high and match the approximate width of their associated channel. The lobes generally have slopes of around 1 or 2° and hummocky surfaces. In front of the Kantbreen ice margin some larger lobes occur independently of any channels. The lobes are up to 700 m long, partly superimpose each other and have a cumulative width of 1800 m. Type-B channels are between 50 and 150 m wide, between 2 and 5 m deep, and 100–500 m long. They are mostly symmetrical in cross-section with rounded edges and along-channel slopes of around 10° (Fig. 4j, k). They often occur in clusters where they cross-cut or merge with each other.

The channels often occur in association with meltwater streams exiting the glaciers and ice caps around Lomfjorden, which makes it likely that they represent channels formed from erosion by downslope processes. The Type-A chan-

nels and their associated lobe-deposits are interpreted as products of mass-transport events occurring along the fjord walls, comparable to those documented in Isfjorden in west Spitsbergen (Forwick & Vorren, 2011). The slope failures are likely triggered by the high supply of relatively fine-grained sediments, delivered into the fjord by rivers and meltwater streams, which rapidly settle and cause slope oversteepening (e.g. Gilbert, 1982; Forwick & Vorren, 2011). The Type-A channels in Lomfjorden probably represent the head scarp, where the slide or slump originated, and the slippery zone of transport, where sediment was continuously eroded. This sediment was then re-deposited at the foot of the slope as large sediment lobes once flow momentum ceased. The hummocky surface of these lobes might derive from the formation of pressure ridges, or from the transport and re-deposition of larger sediment blocks (cf. Prior et al., 1984). In front of Kantbreen the lobes probably represent glacier contact fans formed by the same processes as their adjoining debris lobes in front of Glintbreen (see section 4.1.4). The absence of sediment lobes at the foot of the Type-B channels indicates that the main formation mechanism for these channels is the erosion of the fjord walls by the inflowing meltwater streams, although excavation may have been aided by occasional mass-transport events.

4.1.7. Small Circular Depressions and Elongate Furrows – Iceberg Ploughmarks

Abundant small circular depressions in Lomfjorden are up to 2 m deep with diameters of between 20 and ~80 m. These depressions are U- or V-shaped in cross-section and can be symmetrical or asymmetrical with predominantly gentle slopes (Fig. 4l, m). They often show an up-standing rim on one side. The majority of these features have smooth, defined edges. A few occur as single features or small clusters, but the majority appear at one end of elongated furrows, which commonly occur on bathymetric highs (Fig. 2). These furrows

form criss-crossing patterns and appear in water depths down to 50 m (Fig. 4l). Single furrows are up to 700 m long, <1 m deep and up to 30 m wide (Fig. 4l, m). The furrows have random orientations and often show a linear or curvilinear appearance in planform (Figs. 2, 4l).

The furrows are interpreted as iceberg ploughmarks, formed when the keels of grounded icebergs erode the seafloor into elongate furrows (e.g. Belderson et al., 1973; Dowdeswell et al., 1993; Dowdeswell & Bamber, 2007). This process is frequently observed in front of marine-terminating glaciers (Barnes & Lien, 1988; Woodworth-Lynas & Guigné, 1990). As iceberg drift is largely dependent on wind and ocean currents, changes in the icebergs' direction are common and account for the curvilinear appearance of the ploughmarks (e.g. Dowdeswell & Bamber, 2007; Andreassen et al., 2008). Their occurrence in water depths down to 50 m suggests that the keels of icebergs in Lomfjorden are generally shallower than 50 m (cf. Dowdeswell & Forsberg, 1992; Dowdeswell et al., 1993). The circular depressions at the end of the furrows probably record the in-situ melting of grounded icebergs when movement ceased. Nevertheless, especially where these depressions are detached from the furrows, they could also be pockmarks, which are defined as concave, subaquatic depressions formed as a result of gas or pore fluid seepage (e.g. Harrington, 1985; Hovland & Judd, 1988; Forwick et al., 2009; Roy et al., 2015).

4.2. Seismostratigraphy

Six acoustic facies AF1–AF6 are distinguished in Lomfjorden (Fig. 5).

AF1, is stratigraphically the lowermost facies and inferred to be the oldest. It is acoustically semi-opaque to transparent with only rare internal reflections and is bounded by a hummocky upper reflection of variable strength (Fig. 5). Facies AF1 occasionally crops out on the seafloor, where it is overprinted by

1–3 m high bumps of Facies AF2. The minimum thickness is ∼7.5 m.

Its stratigraphic position, its acoustic appearance and its hummocky upper boundary indicate that AF1 represents the acoustic basement in Lomfjorden, which could either reflect bedrock or glacial till (cf. Forwick et al., 2010; Forwick & Vorren, 2011; Kempf et al., 2013; Roy et al., 2014). Based on the frequent appearance of bedrock on the seafloor as imaged on the multibeam data (section 4.1.1), we consider it more likely that AF1 represents bedrock.

AF2 occurs mostly as small mounds overprinting Facies AF1 (Fig. 5). AF2 is acoustically semi-opaque to transparent, with very weak, chaotic internal reflections that weaken and disappear with depth. AF2 is acoustically similar to AF1, but is bounded by a strong, sharp, and mostly continuous upper reflection and is up to 26 m thick. It directly overlies AF1 (Fig. 5).

AF2 is acoustically similar to subglacial till in Grønfjorden, Isfjorden, Tempelfjorden/Sassenfjorden, Norseliusdjupet, and Van Keulenfjorden (Forwick & Vorren, 2011; Kempf et al., 2013). The overall massive acoustic appearance as well as the loss of internal reflections with depth are thought to indicate uniformly mixed material, possibly of diamictic composition (cf. Stewart & Stoker, 1990; Forwick & Vorren, 2011), which is consistent with an interpretation as glacial till. Furthermore, the bumps of AF2 on the chirp data correlate with the small recessional moraines, some of the De Geer moraines, and glacial lineations on the bathymetric data, also supporting an interpretation as glacial till.

AF3 is acoustically (semi-)transparent with occasional diffuse internal reflections. Based on geometry and appearance, AF3 is sub-divided into two subfacies, AF3a and AF3b. AF3a occurs as lens-shaped bodies in the inner and central fjord (Fig. 5), which can be up to 350 m wide and around 8 m thick. AF3a often pinches out laterally and appears interbedded with AF4, particularly in the inner fjord. AF3b is characterised by a strong, continuous, undulating

bottom reflection and is laterally extensive over large areas in Lomfjorden (Fig. 5). It is more common in the central and outer fjord where it appears as 1–3 m thick packages.

The massive, (semi-)transparent acoustic signature of AF3 is in accordance with mass-transport deposits documented on subbottom profiler data from other areas around Svalbard (e.g Plassen et al., 2004; Forwick & Vorren, 2007; Hogan et al., 2010; Streuff et al., 2015). We thus interpret the lenticular bodies of AF3a as the mass-transport-derived sediment lobes described in section 4.1.6, an interpretation supported by the correlation of the chirp and bathymetric data. The erosional lower contact of AF3b indicates that this subfacies is also a product of mass-transport. The orientation and undulating appearance of this lower boundary in the central fjord suggests the deposits may be related to ice-marginal processes from the tributary glaciers Skinfaksebreen or Gullfaksebreen, and mass-transport from side-walls in the central fjord.

AF4 is acoustically stratified due to the presence of very regular, mostly continuous, parallel internal reflections (Fig. 5). AF4 occurs in the entire fjord, but is particularly common in proximal areas and in bathymetric depressions where it is up to 12 m thick and conformably overlies AF1 or AF3a (Fig. 5).

The stratified acoustic appearance of AF4 suggests regular changes in lithology or density (cf. Syvitski, 1989; Forwick & Vorren, 2011). Similar sediments described from other Spitsbergen fjords have been interpreted as glacimarine sediments derived from suspension settling from meltwater plumes (e.g. Plassen et al., 2004; Kempf et al., 2013; Streuff et al., 2015), or as ice-proximal glacimarine fans in which suspension settling alternates with turbidity currents and gravitational down-slope processes (e.g. Sexton et al., 1992; Forwick & Vorren, 2011). Based on the lithological evidence, we favour the latter interpretation as the most likely mode of formation of this acoustic facies, and suggest an

ice-proximal origin for AF4 (see also section 4.4 below).

AF5 is similar to AF3 with an acoustically semi-transparent appearance and very weak chaotic internal reflections. AF5 occasionally shows a draping character and is common in basins, where it generally overlies AF4 (Fig. 5). It is up to 13 m thick and lacks distinct contacts.

The chaotic internal reflections and acoustic transparency of AF5 indicate fairly homogeneous, possibly fine-grained, material (e.g. Forwick & Vorren, 2011). The draping character and large thickness of AF5 is consistent with sediments deposited in a relatively low-energy glacimarine environment. Although the sediments could also derive from the suspension load carried in rivers or from normal hemipelagic sedimentation from the water column, we consider the rainout of the fine-grained suspension load from meltwater plumes most likely (see also 4.4 below). AF5 is particularly thick in proximal areas of the fjord, thus supporting a glacigenic origin.

AF6 is bounded by the seabed on top and has a stratified acoustic appearance imparted by parallel, opaque internal reflections, whose strength decreases with depth (Fig. 5). AF6 is bounded by a strong bottom reflection in places, which is orientated obliquely to the seabed, but as this reflection cannot be traced for long distances, AF6 can only be unambiguously identified in the central fjord, close to core GC09 (Figs. 5, 9).

The stratigraphic position of AF6 directly beneath the seabed indicates that this facies was only deposited recently and we therefore interpret it as Holocene glacimarine or hemipelagic sediments delivered into the fjord by meltwater streams and tidal processes. Indeed, AF6 is acoustically and lithologically similar to AF4 (see also section 4.4 below). This suggests a similar origin for both facies and would indicate that AF6 was also deposited in a relatively ice-proximal environment.

4.3. Oceanography

CTD data were obtained at three sites in Lomfjorden (Table 1) and are shown in Figure 6. Generally, predominant water masses are colder and fresher in the inner fjord, but warmer and more saline in the outer fjord (Fig. 6), which is likely related to increased run-off of relatively fresh, cold meltwater in the inner fjord. Towards the outer fjord, further away from the glacier fronts, a decreasing influence of meltwater on the water column is seen in the warmer and more saline waters. Water masses with a salinity of <34.4 psu and between 34.4 and 34.9 psu are defined as Polar and Arctic Surface Water, respectively (Ślubowska-Woldengen et al., 2007) and characterise bottom waters in central Lomfjorden (Fig. 6). In the outer fjord Arctic Surface water overlies the warmer, more saline bottom water, whose characteristics are comparable to those reported from the Atlantic Layer in northern Svalbard (part of the Svalbard branch; Aagaard et al., 1987; Pfirman et al., 1994; Ślubowska et al., 2005). A relatively thin superficial layer of colder and fresher water in the outer fjord (Fig. 6) may represent meltwater inflow from Valhallfonna. The inflow of Atlantic water into the inner fjord is probably prevented by the shoaling seafloor. The data suggest (1) that Atlantic water flows into Hinlopenstretet and into Lomfjorden from the northern Svalbard shelf (Ślubowska et al., 2005) and (2) that oceanographically Lomfjorden is not much colder than the fjords in west Spitsbergen (cf. e.g. Svendsen et al., 2002; Ślubowska-Woldengen et al., 2007; Rasmussen et al., 2012).

4.4. Lithostratigraphy

Based on variations in colour, grain size and geographical distribution of sediment in the seven gravity cores analysed, five lithofacies (LF1–LF5) are distinguished in Lomfjorden. Their occurrence in the sediment cores, along with

water content, magnetic susceptibility and grain size distribution, is shown in Figure 7, while examples of x-radiographs and colour photographs are displayed in Figure 8.

LF1 is composed of finely stratified silt with a small but variable clay component and a water content around 30%. Grain size analysis shows that >90% of the sediment is finer than 63 μm and the magnetic susceptibility shows minor variations between overall values from 20 to 40 x 10^{-5} SI (Fig. 7). The sediments are heavily bioturbated and occasional clasts, shells and shell fragments are scattered throughout. Black mottles are abundant (Fig. 8). The silt of LF1 varies in colour between dark grey and dark greyish brown, but very dark grey to black mottles make the sediments appear darker in places (Fig. 8).

The high amount of bioturbation and biogenic activity, indicated by the mottles and shell fragments, suggest favourable living conditions for marine fauna, while the clasts reflect ice-rafted debris settling from melting sea ice and/or icebergs. We thus interpret LF1 as distal glacimarine sediment deposited from suspension rainout from meltwater plumes and/or the water column (hemipelagic sedimentation), combined with bioturbation. A similar lithofacies was also reported in other Spitsbergen fjords by Elverhøi et al. (1983), Plassen et al. (2004), Baeten et al. (2010), and Forwick et al. (2010). LF1 correlates with AF5 (Fig. 9).

LF2 contains massive sand intermixed with variable amounts of silt (Figs. 7, 8). All grain sizes from very coarse sand to silt appear in an upward-fining succession, but the sediments are generally poorly sorted. Coarser components appear slightly darker than finer grains with colours between very dark and dark grey (Fig. 8). The water content is ∼15% and the magnetic susceptibility around 30 x 10^{-5} SI (Fig. 7).

The sand is inferred to have been deposited in an environment with initially high (coarser grains) but increasingly low depositional energy (finer grains). A

succession such as the one observed in LF2 is, for example, common for turbidites (e.g. Gilbert, 1982; Andersen et al., 1996; Syvitski et al., 1996; Lønne, 1997). LF2 is confined to the lowermost centimetres of GC10, and its thickness as well as inaccuracy between time-depth conversion (see section 3) makes unambiguous correlation to an acoustic facies difficult. We tentatively suggest that LF2 forms part of AF3b, which would be in accordance with the previous interpretations of AF3 as mass-transport deposits.

LF3 contains partly compacted, massive, dark grey, fine to medium sand which occurs as lenses, thin horizons, or larger sand bodies in all cores in Lomfjorden except GC12 (Figs. 7, 8). Contacts with surrounding facies range from sharp to gradational. The sand may contain various amounts of silt, but is generally well-sorted with up to 90% of the sediment finer than 63 μm. The water content is <20% and the magnetic susceptibility between 10 and 20 x 10^{-5} SI (Fig. 7). LF3 is interpreted as a product of down-slope gravitational processes. The massive appearance and the presence of silt may indicate intermixing of coarser and finer material and could thus be evidence for sediment reworking, which, in addition to the often sharp contacts, is in good agreement with an interpretation as mass-transport deposits (e.g. Forwick & Vorren, 2007). Where contacts are more gradual, emplacement of the sand could relate to non-eroding turbidity flows or hydroplaning debris flows (cf. e.g. Elverhøi et al., 2000; Mulder & Alexander, 2001; Forwick & Vorren, 2007, 2011). Sand appearing as thicker packages probably derives from larger-scale events, such as slope failures along the fjord walls or glacier outwash (cf. e.g. Boulton, 1986; Forwick & Vorren, 2007), whereas thinner strata may represent small-scale events, such as turbidites. We correlate LF3 with acoustic facies AF3 (Fig. 9).

LF4 is divided into subfacies LF4a and LF4b. LF4a comprises very weakly stratified clay with variable amounts of silt which occasionally contain lenses of

LF3 (Fig. 7). The stratification is mainly imparted by colour changes from grey to (dark) greyish brown. Grain size analyses reveal that >95% of the sediment is finer than 63 μm (Fig. 7). LF4a contains occasional clasts and abundant mottles (Fig. 8). Its magnetic susceptibility is generally between 10 and 20 x 10^{-5} SI, and the water content is around 50% (Fig. 7). LF4b occurs only in GC10, and contains the clay from LF4a interbedded with thin sandy beds of LF3 (Fig. 8). The latter have relatively sharp bottom and graded top contacts, can appear contorted, are relatively well-sorted, and show a weak tendency of cross-bedding (Figs. 7, 8).

LF4a is similar to glacimarine muds documented from other Spitsbergen fjords (e.g. Forwick & Vorren, 2009; Kempf et al., 2013; Streuff et al., 2015), which suggests that the clay and silt originate from the rainout of suspension load carried in glacial meltwater plumes. The weak stratification is indicative of a depositional environment with low energy, which could stem from regular variations in sediment source, sediment delivery and discharge, or glacier front oscillations (e.g. Ó Cofaigh & Dowdeswell, 2001; Szczuciński & Zajaczkowski, 2012). The regularity of the lamination suggests seasonal changes to be the cause for such variations. Based on the characteristics of the sand layers, LF4b is interpreted as suspension rainout alternating with turbidites (e.g. Gilbert, 1982; Mackiewicz et al., 1984; Ó Cofaigh & Dowdeswell, 2001). LF4a correlates with acoustic facies AF6, whereas LF4b probably reflects the stratified nature of AF4 (Fig. 9).

LF5 is subdivided into LF5a and LF5b. LF5a consists of soft, weakly laminated, brown to dark grey clayey silt. Laminations occur due to minor colour variations between brown and dark grey, as well as density variations (Fig. 8), the latter probably related to small changes in clay content. More than 90% of the sediment is finer than 63 μm. The water content is between 20 and 30% and the magnetic susceptibility shows minor oscillations with values between 10 and

30 x 10^{-5} SI. LF5a is prominent in inner Lomfjorden and occurs in the proximal cores (Fig. 7). Occasional shells, shell fragments and abundant mottles appear throughout. In GC05 and GC07 the silt from LF5a is interbedded with several mm- to cm-thick well-sorted sand horizons of LF3, which have sharp bottom boundaries and show occasional cross-bedding (Fig. 8). This subfacies is defined as LF5b (Fig. 7).

The fine grain size of the sediments in LF5a indicates a low-energy depositional environment and is similar to LF4a, and to glacimarine muds from other Spitsbergen fjords. We therefore interpret this lithofacies as glacimarine sediment deposited by suspension rainout from meltwater plumes exiting a tidewater glacier (cf. Elverhøi et al., 1980, 1983; Plassen et al., 2004; Forwick & Vorren, 2009; Kempf et al., 2013; Streuff et al., 2015). Similar to LF4a, the laminations may reflect regular, probably seasonal changes in meltwater and sediment supply (cf. Cowan & Powell, 1990; Powell & Domack, 1995). LF5a is slightly coarser than LF4a, with an increased proportion of silt, which suggests that LF5a was deposited in a slightly higher-energy environment than LF4a and thus reflects more proximal conditions. We infer similar processes of formation for LF5b as for LF4b and suggest that LF5b consists of glacimarine muds deposited from suspension settling alternating with turbidites and/or other mass-transport deposits. LF5 forms part of the acoustic facies AF4, with the acoustic stratification probably reflecting the common occurrence of turbidites in LF5b (Fig. 9).

4.5. Radiocarbon dates and sediment accumulation rates

AMS radiocarbon dating was carried out on foraminifera and bivalves from five sediment depths in core GC12 in outer Lomfjorden, and from two sediment depths from GC08 in the central fjord (Table 2, Fig. 10). All radiocarbon dates were taken from lithofacies LF1. A basal age of 9.7 cal ka BP from GC12 shows

that the sedimentary record in this core covers a large part of the Holocene. Conventional radiocarbon ages were used to calculate sediment accumulation rates (SARs), which, in GC12, decrease up-core, and range from 0.72 to 0.21 mm a^{-1} (Fig. 10). In GC08, a basal date of ∼4.5 cal ka BP at 265 cm and a date of ∼2 cal ka BP at 207 cm provide a low SAR of 0.3 mm a^{-1} (Fig. 10), which indicates relatively ice-distal conditions during the accumulation of LF1 in this core (cf. e.g. Elverhøi et al., 1980, 1983). Note that these rates are based on an assumption of linear sediment accumulation.

Table 2: Radiocarbon dates and calibrated ages used in this study.

Core ID	Depth [cm]	Lab Code	Sample	Reported age [^{14}C a BP]	Mean probability age [cal a BP]	2σ [cal a BP]
GC08	207	Beta–441327	Bivalve	2490 ± 30	2021	2146–1882
GC08	265	Beta–441328	Foraminifera	4420 ± 30	4452	4595–4293
GC12	20	Beta–441322	Foraminifera	940 ± 30	470	543–357
GC12	105	Beta–441323	Foraminifera	4090 ± 30	3996	4139–3849
GC12	180	Beta–441324	Foraminifera	6340 ± 30	6689	6824–6555
GC12	240	Beta–441325	Bivalve	7890 ± 30	8258	8360–8156
GC12	328	Beta–441326	Bivalve	9120 ± 30	9696	9872–9540

5. Discussion

5.1. Glacial geomorphology and landform assemblages in Lomfjorden

Swath-bathymetric data from Lomfjorden reveal (1) bedrock highs, (2) glacial lineations, (3) drumlins, (4) recessional and De Geer moraines with, in some cases, associated debris lobes, (5) submarine channels, (6) mass-transport deposits, and (7) iceberg ploughmarks. Except for the bedrock highs, which have been at least partly modified by glacial streamlining, all of the landforms are regarded as glacigenic, i.e. formed from subglacial, ice-marginal, or glacimarine processes. They are common components of glacial landform assemblages doc-

umented in other Svalbard fjords (cf. Boulton, 1986; Solheim & Pfirman, 1985; Solheim, 1991; Plassen et al., 2004; Ottesen & Dowdeswell, 2006; Ottesen et al., 2008; Baeten et al., 2010; Forwick & Vorren, 2011; Kempf et al., 2013; Flink et al., 2015; Streuff et al., 2015). Based on their orientation within the fjord, the landforms in Lomfjorden can be divided into two separate assemblages: (1) the Trunk Glacier Assemblage, formed from an extended Veteranen glacier flowing through the fjord, parallel to the fjord long axis, and (2) the Tributary Glacier Assemblage, formed from glaciers flowing into the fjord from the sides, i.e. perpendicular to the fjord long axis (Fig. 11).

5.1.1. Trunk Glacier Assemblage

The glacial lineations, drumlins, De Geer moraines, and recessional moraines in central Lomfjorden are part of the Trunk Glacier Assemblage (Fig. 11). Their orientation is parallel or transverse to the main fjord axis, which implies that these landforms are related to trunk-ice flowing through the fjord from south to north, and were thus deposited by an extended Veteranen glacier. The absence of terminal moraines in this assemblage suggests only one glacial advance-retreat sequence, and we infer that the glacial lineations and drumlins formed during ice advance, possibly beneath fast-flowing ice (cf. King et al., 2009), and that the recessional and De Geer moraines formed during episodic ice retreat (cf. Dowdeswell et al., 2010; Hogan et al., 2010).

5.1.2. Tributary Glacier Assemblage

The Tributary Glacier Assemblage contains all recessional moraines located in front of the tributary glaciers and, in some cases, debris lobes associated with the outermost moraine (Fig. 11). It can be further sub-divided into three individual landform assemblages related to the three tributary glaciers Valhallfonna in the outer fjord, Frøyabreen on the eastern shore and Glintbreen/Kantbreen in the

inner fjord (the "tributaries", Fig. 11). The landforms are orientated transverse to the respective glacier's direction of ice flow, i.e. (sub-)parallel to the main fjord axis, and are therefore likely a product of individual glacier dynamics, with ice flow occurring more or less perpendicular to that of the trunk glacier. The timing of formation for all landform assemblages is discussed in section 5.3 below.

5.2. Sedimentary environments

From the lithological record in Lomfjorden we infer three main sedimentary processes: (1) suspension rainout from meltwater plumes and/or the water column, (2) delivery of IRD by icebergs and possibly sea ice, and (3) sediment reworking by down-slope gravity flows and iceberg ploughing. In outer and central Lomfjorden, the laminated clayey silt of facies LF1 shows signs of intense biological activity in the form of bioturbation, black mottles, and shell fragments, indicating a distal glacimarine environment (cf. Ó Cofaigh & Dowdeswell, 2001). Ice-distal conditions are further supported by the very low SARs between ∼0.2 and 0.7 mm a^{-1} (cf. Elverhøi et al., 1983; Forwick & Vorren, 2009; Szczuciński et al., 2009; Streuff et al., 2015). Note that these rates are up to one order of magnitude lower than rates suggested for glacier-distal environments in other Spitsbergen fjords (Elverhøi et al., 1980, 1983), and are more similar to SARs documented from east Greenland. This could indicate that meltwater availability was much lower during the Holocene, that glacial erosion was too weak to produce sufficient "rock flour", and/or that the glacimarine environment of east Spitsbergen is indeed colder and more polar compared to that of the warmer, more temperate, west Spitsbergen (cf. Mackiewicz et al., 1984; Dowdeswell et al., 1998; Ó Cofaigh & Dowdeswell, 2001). As colder conditions in Lomfjorden are inconsistent with the CTD data, which record the inflow of warm Atlantic water

into the fjord, based on the assumption that glaciers in west and east Spitsbergen would produce similar amounts of rock flour (cf. Dallmann et al., 2002), a low sediment accumulation rate during the Holocene must thus be a consequence of decreased meltwater runoff. The occurrence of only LF1 in GC12 and its basal date of 9.7 cal ka BP shows that the sedimentary processes at this location remained largely unchanged throughout the Holocene. In the central fjord, the laminated silts of LF1 at the base of GC08 also reflect ice-distal conditions until after ∼2.0 cal ka BP, deposited at a SAR of 0.3 mm a^{-1}. The upwards fining of LF1 in the central and inner fjord into the weakly laminated clay of LF4a could suggest increasingly distal conditions and thus continuous glacier retreat, which is also indicated by the decreasing SARs in GC12 (cf. Syvitski & Murray, 1981; Gilbert, 1982; Elverhøi et al., 1983; Sexton et al., 1992). However, occasional sand bodies with sharp bounding contacts attest to the occurrence of down-slope mass-transport processes in Lomfjorden, and the concurrent occurrence of LF4a with larger bodies and smaller lenses of LF3 at the top of GC08 and GC09 thus shows an increasing frequency of mass-transport events in recent times. This could be related to a more proximal depositional environment, possibly related to a late Holocene glacier re-advance, which is also implied by the presence of the acoustically stratified sediments of AF6 (see section 4.2).

In cores GC05, GC06, and GC07 in the inner fjord clayey silt is interbedded with sandy turbidites, providing evidence for relatively proximal conditions (e.g. Gilbert, 1982; Gilbert et al., 1993). The decreasing frequency of the sandy layers up-sequence could be related to decreasing depositional energy and increasingly ice-distal conditions as a consequence of ice retreat. Nevertheless, a lack of turbidites could also be related to decreasing meltwater, and thus sediment, availability (cf. Mackiewicz et al., 1984; Stevens, 1990; Laberg & Vorren, 1995; Ó Cofaigh & Dowdeswell, 2001), which may be a consequence of a period of

generally cooler conditions and glacier advance.

Most areas in the fjord are influenced by intense sediment reworking, either due to erosion and re-deposition from meltwater streams along the submarine channels, due to down-slope gravitational flows forming mass-transport deposits, or due to ploughing by icebergs calved from the local tidewater glaciers. However, as icebergs are absent on recent aerial photos from the fjord, iceberg ploughing does not appear to play a major role in contemporary sediment reworking.

5.3. Glacial evolution in Lomfjorden

The Trunk Glacier Assemblage records a single glacial advance-retreat event related to the flow of an extended Veteranen glacier along the length of Lomfjorden. Fjord-parallel glacial lineations occurring throughout the fjord indicate formation during a time when Lomfjorden was fully glaciated. We infer that all the landforms in the Trunk Glacier Assemblage were formed from ice-streaming during and after the Last Glacial Maximum. This interpretation is supported by the fact that the sediment core GC12 in the outer fjord provides evidence for continuously ice-distal conditions since at least 9.7 cal ka BP, and that the landforms in the Trunk Glacier Assemblage are consistent with those formed by other palaeo-ice streams in eastern Svalbard (Dowdeswell et al., 2010; Hogan et al., 2010; Ingólfsson & Landvik, 2013). Lomfjorden may thus have served as one of the larger fjord systems channelling a fast-flowing ice stream from the Svalbard-Barents Sea Ice Sheet during the LGM, the latter presumably serving as a tributary to the ice stream draining the ice sheet from south to north through Hinlopenstretet (e.g. Landvik et al., 1998; Ottesen et al., 2007; Ingólfsson & Landvik, 2013). The basal date from GC12 also provides the first documented age for the deglaciation of northeast Spitsbergen and indicates that

deglaciation was underway by 9.7 cal ka BP. It is important to note, however, that this is a minimum age for two reasons: (1) by this time the ice margin must have already retreated far into the fjord, as shown by the presence of only ice-distal sediments in GC12, and (2) GC12 only covers the uppermost 3.36 m of a ∼18 m-thick sedimentary basin infill sequence (Fig. 10). This strongly suggests that Lomfjorden was ice-free much earlier than other Spitsbergen fjords, which is also indicated by recent work from Ingólfsson et al. (2016), who suggest that De Geerbukta (see Fig. 1) must have been deglaciated before 12.0 cal ka BP. The succession of the ice-proximal stratified sediments from AF4 at the bottom of the basin, which are overlain by the ice-distal massive sediments of AF5 at the core site of GC12 (Fig. 10), suggests that retreat from the core site was relatively continuous and unlikely to have been interrupted by a glacier re-advance during the Holocene. This is supported by the continuous, roughly exponential decrease in sediment accumulation rate in GC12 (Fig. 10). The latter also shows that the assumption of linear sediment accumulation would be incorrect, preventing the calculation of a more accurate deglaciation age. The basal age of ∼4.5 cal ka BP in ice-distal sediments from GC08 shows that the glaciers must have been well south of the core site by this time. Considering the very limited fjord width ($<$ 3 km) at the core site of GC08 and, as a consequence, the concentrated sediment input from a minimum of three glaciers, this implies that the margins of most of the glaciers were located on land, likely at considerable distances from the coast during the deposition of LF1.

An early and extensive deglaciation of Lomfjorden yields two major implications: (1) If the outer parts of Lomfjorden were indeed ice-free before 12 cal ka BP (cf. Ingólfsson et al., 2016), the inferred position of the ice margin would be somewhere in the central part of Lomfjorden or even further south around that time. This is at odds with previous reconstructions of the extent of the

Svalbard-Barents Sea Ice Sheet, which place the ice margin ∼60 km north at the northern entrance of Hinlopenstretet around 12 cal ka BP (e.g. Landvik et al., 1998; Ingólfsson & Landvik, 2013). This suggests that these reconstructions need to be revised as more data emerges from east Spitsbergen. (2) As the onset of deglaciation in west Spitsbergen was dated to around 15 cal ka BP, with ice having receded into the fjords around 12 cal ka BP and fjords being ice-free around 10 cal ka BP (e.g. Landvik et al., 1998; Ingólfsson & Landvik, 2013), our data imply that the deglacial evolution of Lomfjorden could have been similar to that of fjords from west Spitsbergen. This seems reasonable, given the apparent similarity in their oceanography (see section 4.3). A warmer setting than originally thought for Lomfjorden is also supported by the very extensive retreat of the glaciers documented from our sediment cores. Although the latter is at odds with glaciers in west Spitsbergen, one explanation could be that Lomfjorden is located further inland than most west Spitsbergen fjords, and has a presumably drier climate. This may have led to reduced precipitation and, as a consequence, to increasingly negative glacier mass balances throughout most of the deglaciation.

In contrast to the Trunk Glacier Assemblage, the landforms of the Tributary Glacier Assemblage must have formed in an ice-free fjord, as the presence of a trunk glacier in the fjord would presumably have prevented formation of the observed landforms. The Tributary Assemblages are consistent with landform assemblages observed in front of other Spitsbergen tidewater glaciers, where large outer moraines and a succession of recessional or annual push moraines are generally associated with Holocene re-advance, followed by slow and stepwise retreat, either related to a glacier surge, or to the LIA cooling (e.g. Plassen et al., 2004; Ottesen & Dowdeswell, 2006; Forwick & Vorren, 2011; Flink et al., 2015; Streuff et al., 2015). It is thus possible that the Lomfjorden tributaries

underwent re-advance during the Holocene, which also seems to be indicated by the lithological evidence. We note that none of the Lomfjorden glaciers are recognised as surge-type at present (Hagen, 1993), and, hence, the slightly larger outer moraines could represent the glaciers' maximum extents during the LIA (Forwick & Vorren, 2011, and references therein). However, the presence of the outermost recessional moraines at 1500 m (Valhallfonna), 200 m (Frøyabreen), and 220 m (Glintbreen/Kantbreen) from the present glacier termini show that such glacier advances cannot have been very extensive. This is further supported by the relatively small dimensions of the terminal moraines. Alternatively, small terminal moraines and the relative lack of turbidites in the upper parts of all proximal cores could also be related to moraine formation during deglaciation and associated ice retreat as the tributary glaciers decoupled from the Veteranen ice stream. This explanation seems reasonable as all landforms in the Tributary Glacier Assemblage occur in shallow waters very close to the present coast. The larger moraines and associated debris lobes in front of Glintbreen/Kantbreen and Valhallfonna could then have formed during a prolonged still-stand related to ice grounding close to the shallow coastline (cf. e.g. Crossen, 1991; Seramur et al., 1997; Ó Cofaigh, 1998; Ó Cofaigh et al., 1999).

Considering that most Svalbard glaciers experienced at least one, usually relatively extensive, re-advance during the Holocene, and that these advances left distinct geomorphological imprints in the submarine record (cf. Plassen et al., 2004; Ottesen & Dowdeswell, 2006; Baeten et al., 2010; Forwick & Vorren, 2011; Kempf et al., 2013; Flink et al., 2015; Streuff et al., 2015), the absence of similarly distinct and extensive assemblages in Lomfjorden is notable. However, the glaciers in Lomfjorden likely retreated far behind their present positions during deglaciation, as indicated by the large proportion of distal sediments in GC08. Hence the glacier margins would not necessarily have advanced far into

the fjord during their respective LIA advances. Indeed, the presence of terrestrial moraines in front of most land-terminating glaciers in the area (see Fig. 1) shows that the minority of glaciers reached tidewater during the LIA. Alternatively, the generally drier continental climate in eastern Spitsbergen may not have supplied sufficient precipitation, causing any LIA advances in Lomfjorden to be restricted.

6. Conclusions

Swath-bathymetric data from Lomfjorden provide the first insights into glacigenic landform-sediment assemblages in east Spitsbergen fjords. The landforms are: (1) streamlined bedrock highs, (2) glacial lineations, (3) drumlins, (4) recessional moraines and, in some cases, associated debris lobes, (5) De Geer moraines (6) submarine channels and mass-transport deposits, and (7) iceberg ploughmarks. We suggest that Lomfjorden was fully glaciated during the LGM and channelled a fast-flowing ice stream, which coalesced with the ice stream flowing through Hinlopenstretet at the mouth of the fjord. Drumlins and lineations record the advance of the ice stream through the fjord with recessional moraines and De Geer moraines recording slow and step-wise retreat. A radiocarbon date of ∼9.7 cal ka BP in ice-distal sediments from the outer fjord suggests that deglaciation was well underway by this time. The inner parts of the fjord were ice-free before ∼4.5 cal ka BP and by this time all glaciers had retreated far into the hinterland. Our findings indicate that the glaciers in Lomfjorden may have undergone more extensive retreat during deglaciation than glaciers in west Spitsbergen. We suggest that this was likely caused by a drier climate and the resulting negative mass balances.

The principal sedimentary processes after deglaciation were (1) suspension settling from meltwater (plumes) and from the water column, and (2) reworking of

the sediments by (a) gravitational mass-flow events and (b) iceberg ploughing. Deposition of partly bioturbated clayey silt occurred from suspension settling in ice-distal areas at decreasing sediment accumulation rates from 0.7 to 0.2 mm a^{-1}; the clayey silts are overlain by silty clay recording progressive glacier retreat. Silty clay interbedded with frequent sandy turbidites in the inner fjord indicates a higher-energy depositional environment, possibly related to more proximal glacimarine conditions. Ice-rafting played a minor role and delivered occasional lonestones to the outer fjord. Throughout the Holocene submarine channels formed from erosion by meltwater streams flowing into the fjord, which led to the deposition of numerous mass-transport deposits. The reworking of glacimarine sediment by grounded iceberg keels resulted in the formation of abundant iceberg ploughmarks during deglaciation. During the LIA, the local tidewater glaciers underwent (restricted) re-advances, and either formed terrestrial moraines, or submarine terminal moraines very close to the coast.

Acknowledgments

This work, as part of the GLANAM project "Glaciated North Atlantic Margins", was funded by the People Programme (Marie Curie Actions) of the European Union's Seventh Framework Programme FP7/2007-2013/ under REA grant agreement n^{o}317217. We thank the captain and crew of *R/V Helmer Hanssen*, Kelly Hogan, the students of the UNIS course AG211, and Oscar Fransner and Anne Flink for their help with data acquisition. Discussions with Anne Flink, Elena Grimoldi and Wesley Farnsworth as well as the comments of two anonymous reviewers were greatly appreciated and further helped to improve the manuscript.

References

Aagaard, K., Foldvik, A., & Hillman, S. (1987). The West Spitsbergen Current: disposition and water mass transformation. *Journal of Geophysical Research: Oceans*, *92*, 3778–84. doi:10.1029/JC092iC04p03778.

Andersen, E., Dokken, T., Elverhøi, A., Solheim, A., & Fossen, I. (1996). Late Quaternary sedimentation and glacial history of the western Svalbard continental margin. *Marine Geology*, *133*, 123–56. doi:10.1016/0025-3227(96)00022-9.

Andreassen, K., Laberg, J., & Vorren, T. (2008). Seafloor geomorphology of the SW Barents Sea and its glaci-dynamic implications. *Geomorphology*, *97*, 157–77. doi:10.1016/j.geomorph.2007.02.050.

Baeten, N., Forwick, M., Vogt, C., & Vorren, T. (2010). Late Weichselian and Holocene sedimentary environments and glacial activity in Billefjorden, Svalbard. *Geological Society, London, Special Publications*, *344*, 207–23. doi:10.1144/SP344.15.

Barnes, P., & Lien, R. (1988). Icebergs rework shelf sediments to 500 m off Antarctica. *Geology*, *16*, 1130–3. doi:10.1130/0091-7613(1988).

Beaudry, L. M., & Prichonnet, G. (1991). Late Glacial De Geer moraines with glaciofluvial sediment in the Chapais area, Québec (Canada). *Boreas*, *20*, 377–94. doi:10.1111/j.1502-3885.1991.tb00286.x.

Belderson, R. H., Kenyon, N. H., & Wilson, J. B. (1973). Iceberg plough marks in the northeast Atlantic. *Palaeogeography, Palaeoclimatology, Palaeoecology*, *13*, 215–24. doi:10.1016/0031-0182(73)90020-5.

Benn, D., & Evans, D. (2010). *Glaciers and Glaciation*. (2nd ed.). Hodder Education.

Blake, K. (2000). Common origin for De Geer moraines of variable composition in Raudvassdalen, northern Norway. *Journal of Quaternary Science*, *15*, 633–44. doi:10.1002/1099-1417(200009)15:6¡633::AID-JQS543¿3.0.CO;2-F.

Boulton, G. (1986). Push-moraines and glacier-contact fans in marine and terrestrial environments. *Sedimentology*, *33*, 667–98. doi:10.1111/j.1365-3091.1986.tb01969.x.

Boulton, G., Van Der Meer, J., Hart, J., Beets, D., Ruegg, G., Van Der Wateren, F., & Jarvis, J. (1996). Till and moraine emplacement in a deforming bed surge – an example from a marine environment. *Quaternary Science Reviews*, *15*, 961–87. doi:10.1016/0277-3791(95)00091-7.

Burton, D. J., Dowdeswell, J. A., Hogan, K. A., & Noormets, R. (2016). Marginal fluctuations of a Svalbard surge-type tidewater glacier, Blomstrandbreen, since the Little Ice Age: a record of three surges. *Arctic, Antarctic, and Alpine Research*, *48*, 411–26. doi:10.1657/AAAR0014-094.

Cai, J., Powell, R., Cowan, E., & P., C. (1997). Lithofacies and seismic-reflection interpretation of temperate glacimarine sedimentation in Tarr Inlet, Glacier Bay, Alaska. *Marine Geology*, *143*, 5–37. doi:10.1016/S0025-3227(97)00088-1.

Clark, C., Hughes, A., Greenwood, S., Spagnolo, M., & Ng, F. (2009). Size and shape characteristics of drumlins, derived from a large sample, and associated scaling laws. *Quaternary Science Reviews*, *28*, 677–92. doi:10.1016/j.quascirev.2008.08.035.

Clark, C., Tulaczyk, S., Stokes, C., & Canals, M. (2003). A groove-ploughing theory for the production of mega-scale glacial lineations, and implications for ice-stream mechanics. *Journal of Glaciology*, *49*, 240–56. doi:10.3189/172756503781830719.

Cottier, F., Nilsen, F., Skogseth, R., Tverberg, V., Skarðhamar, J., & Svendsen, H. (2010). Arctic fjords: a review of the oceanographic environment and dominant physical processes. *Geological Society, London, Special Publications*, *344*, 35–50. doi:10.1144/SP344.4.

Cowan, E., & Powell, R. (1990). Suspended sediment transport and deposition of cyclically interlaminated sediment in a temperate glacial fjord, Alaska, USA. *Geological Society, London, Special Publications*, *53*, 75–89. doi:10.1144/GSL.SP.1990.053.01.04.

Crossen, K. J. (1991). Structural control of deposition by Pleistocene tidewater glaciers, Gulf of Maine. *Geological Society of America Special Papers*, *261*, 127–36. doi:10.1130/SPE261-p127.

Dallmann, W., Ohta, Y., Elvevold, S., & Blomeier, D. (2002). *Bedrock map of Svalbard and Jan Mayen*. Norsk Polarinstitutt, Temakart No. 33.

De Geer, G. (1940). *Geochronologia suecica principles* volume 18. Almqvist & Wiksells.

Dowdeswell, J., & Bamber, J. (2007). Keel depths of modern Antarctic icebergs and implications for sea-floor scouring in the geological record. *Marine Geology*, *243*, 120–31. doi:10.1016/j.margeo.2007.04.008.

Dowdeswell, J., Elverhøi, A., & Spielhagen, R. (1998). Glacimarine sedimentary processes and facies on the Polar North Atlantic margins. *Quaternary Science Reviews*, *17*, 243–72. doi:10.1016/S0277-3791(97)00071-1.

Dowdeswell, J., & Forsberg, C. (1992). The size and frequency of iceberg and bergy bits derived from tidewater glaciers in Kongsfjorden, northwest Spitsbergen. *Polar Research*, *2*, 81–91. doi:10.1111/j.1751-8369.1992.tb00414.x.

Dowdeswell, J., Hogan, K., Evans, J., Noormets, R., Ó Cofaigh, C., & Ottesen, D. (2010). Past ice-sheet flow east of Svalbard inferred from streamlined subglacial landforms. *Geology*, *38*, 163–6. doi:10.1130/G30621.1.

Dowdeswell, J. A., Villinger, H., Whittington, R. J., & Marienfeld, P. (1993). Iceberg scouring in Scoresby Sund and on the East Greenland continental shelf. *Marine Geology*, *111*, 37–53. doi:10.1111/j.1502-3885.1994.tb00602.x.

Elverhøi, A., Andersen, E., Dokken, T., Hebbeln, D., Spielhagen, R., Svendsen, J., & Forsberg, C. (1995). The growth and decay of the Late Weichselian ice sheet in western Svalbard and adjacent areas based on provenance studies of marine sediments. *Quaternary Research*, *44*, 303–16. doi:10.1006/qres.1995.1076.

Elverhøi, A., Fjeldskaar, W., Solheim, A., Nyland-Berg, M., & Russwurm, L. (1993). The Barents Sea Ice Sheet – A model of its growth and decay during the last ice maximum. *Quaternary Science Reviews*, *12*, 863–73. doi:10.1016/0277-3791(93)90025-H.

Elverhøi, A., Harbitz, C., Dimakis, P., Morhrig, D., Marr, J., & G., P. (2000). On the dynamics of subaqueous debris flows. *Oceanography*, *13*. doi:10.5670/oceanog.2000.20.

Elverhøi, A., Liestøl, O., & Nagy, J. (1980). Glacial erosion, sedimentation and microfauna in the inner part of Kongsfjorden, Spitsbergen. *Norsk Polarinstitutt Skrifter*, *172*, 33–58.

Elverhøi, A., Lønne, Ø., & Seland, R. (1983). Glaciomarine sedimentation in a modern fjord environment, Spitsbergen. *Polar Research*, *1*, 127–50. doi:10.1111/j.1751-8369.1983.tb00697.x.

Flink, A. E., Noormets, R., Kirchner, N., Benn, D. I., Luckman, A., & Lovell,

H. (2015). The evolution of a submarine landform record following recent and multiple surges of Tunabreen glacier, Svalbard. *Quaternary Science Reviews*, *108*, 37–50. doi:10.1016/j.quascirev.2014.11.006.

Forwick, M., Baeten, N., & Vorren, T. (2009). Pockmarks in Spitsbergen fjords. *Norwegian Journal of Geology*, *89*, 65–77.

Forwick, M., & Vorren, T. (2007). Holocene mass-transport activity and climate in outer Isfjorden, Spitsbergen: marine and subsurface evidence. *The Holocene*, *17(6)*, 707–16. doi:10.1177/0959683607080510.

Forwick, M., & Vorren, T. (2009). Late Weichselian and Holocene sedimentary environments and ice rafting in Isfjorden, Spitsbergen. *Paleogeography, Paleoclimatology, Paleoecology*, *280(1)*, 258–74. doi:10.1016/j.palaeo.2009.06.026.

Forwick, M., & Vorren, T. (2011). Stratigraphy and deglaciation of the Isfjorden area, Spitsbergen. *Norwegian Journal of Geology*, *90*, 163–79.

Forwick, M., Vorren, T., Hald, M., Korsun, S., Roh, Y., Vogt, C., & Yoo, K. (2010). Spatial and temporal influence of glaciers and rivers on the sedimentary environment in Sassenfjorden and Tempelfjorden, Spitsbergen. *Geological Society, London, Special Publications*, *344(1)*, 163–93. doi:10.1144/SP344.13.

Gilbert, R. (1982). Contemporary sedimentary environments on Baffin Island, NWT, Canada: Glaciomarine processes in fiords of eastern Cumberland Peninsula. *Arctic and Alpine Research*, *14*, 1–12. doi:10.2307/1550809.

Gilbert, R., Aitken, A., & Lemmen, D. (1993). The glacimarine sedimentary environment of Expedition Fiord, Canadian High Arctic. *Marine Geology*, *110*, 257–73. doi:10.1016/0025-3227(93)90088-D.

Gowan, E. J., Fransner, O. J., & Dowdeswell, J. (2016). ICESHEET 1.0: a pro-

gram to produce paleo-ice sheet reconstructions with minimal assumptions. *Geoscientific Model Development*, *9*, 1673. doi:10.5194/gmd-9-1673-2016.

Hagen, J. (1993). *Glacier atlas of Svalbard and Jan Mayen* volume 129. Norsk Polarinstitutt Middelelser. URL: `http://hdl.handle.net/11250/173065`.

Hald, M., Ebbesen, H., Forwick, M., Godtliebsen, F., Khomenko, L., Korsun, S., & Vorren, T. (2004). Holocene paleoceanography and glacial history of the West Spitsbergen area, Euro-Arctic margin. *Quaternary Science Reviews*, *23(20)*, 2075–88. doi:10.1016/j.quascirev.2004.08.006.

Harrington, P. (1985). Formation of pockmarks by pore-water escape. *Geo-Marine Letters*, *5*, 193–7. doi:10.1007/BF02281638.

Hogan, K. A., Dowdeswell, J. A., Noormets, R., Evans, J., & Ó Cofaigh, C. (2010). Evidence for full-glacial flow and retreat of the Late Weichselian Ice Sheet from the waters around Kong Karls Land, eastern Svalbard. *Quaternary Science Reviews*, *29*, 3563–82. doi:10.1016/j.quascirev.2010.05.026.

Hoppe, G. (1957). Problems of glacial morphology and the Ice Age. *Geografiska Annaler*, (pp. 1–18). doi:10.2307/520339.

Hovland, M., & Judd, A. G. (1988). *Seabed pockmarks and seepages: impact on geology, biology and the marine environment*.

Ingólfsson, Ó., Farnsworth, W., Schomacker, A., Håkansson, L., & Allaart, L. (2016). Younger Dryas-Holocene glacial advance in De Geerbukta, NE Spitsbergen: climate controlled, or glacial system turning to Holocene mode. In *PAST Gateways Abstracts*.

Ingólfsson, O., & Landvik, J. (2013). The Svalbard-Barents Sea ice-sheet – historical, current and future perspectives. *Quaternary Science Reviews*, *64*, 33–60. doi:10.1016/j.quascirev.2012.11.034.

Jones, G. A., & Keigwin, L. D. (1988). Evidence from Fram Strait (78 N) for early deglaciation. *Nature*, *336*, 56–9. doi:10.1038/336056a0.

Kempf, P., Forwick, M., Laberg, J., & Vorren, T. (2013). Late Weichselian – Holocene sedimentary palaeoenvironment and glacial activity in the high-Arctic van Keulenfjorden, Spitsbergen. *The Holocene*, *23(11)*, 1607–18. doi:10.1177/0959683613499055.

King, E., Hindmarsh, R., & Stokes, C. (2009). Formation of mega-scale glacial lineations observed beneath a West Antarctic ice stream. *Nature Geoscience*, *2(8)*, 585–8. doi:10.1038/ngeo581.

Kirchner, N., Ahlkrona, J., Gowan, E. J., Lötstedt, P., Lea, J. M., Noormets, R., von Sydow, L., Dowdeswell, J. A., & Benham, T. (2016). Shallow ice approximation, second order shallow ice approximation, and full Stokes models: A discussion of their roles in palaeo-ice sheet modelling and development. *Quaternary Science Reviews*, *135*, 103–14. doi:10.1016/j.quascirev.2016.01.013.

Kleiber, H., Knies, J., & Niessen, F. (2000). The Late Weichselian glaciation of the Franz Victoria Trough, northern Barents Sea: ice sheet extent and timing. *Marine Geology*, *168*, 25–44. doi:10.1038/ngeo581.

Koç, N., Klitgaard-Kristensen, D., Hasle, K., Forsberg, C., & Solheim, A. (2002). Late glacial palaeoceanography of Hinlopen Strait, northern Svalbard. *Polar Research*, *21*, 307–14. doi:10.1111/j.1751-8369.2002.tb00085.x.

Kristensen, L., Benn, D., Hormes, A., & Ottesen, D. (2009). Mud aprons in front of Svalbard surge moraines: Evidence of subglacial deforming layers or proglacial glaciotectonics? *Geomorphology*, *111(3)*, 206–21. doi:10.1016/j.geomorph.2009.04.022.

Laberg, J., & Vorren, T. (1995). Late Weichselian submarine debris flow deposits on the Bear Island trough-mouth fan. *Marine Geology*, *127*, 45–72. doi:10.1016/0025-3227(95)00055-4.

Landvik, J., Bondevik, S., Elverhøi, A., Fjeldskaar, W., Mangerud, J., Salvigsen, O., Siegert, M. J., Svendsen, J.-I., & O., V. T. (1998). The last glacial maximum of Svalbard and the Barents Sea area: ice sheet extent and configuration. *Quaternary Science Reviews*, *17(1-3)*, 43–75. doi:10.1016/S0277-3791(97)00066-8.

Landvik, J. Y., Hjort, C., Mangerud, J., Moller, P., & Salvigsen, O. (1995). The Quaternary record of eastern Svalbard-an overview. *Polar Research*, *14*, 95–104. doi:10.1111/j.1751-8369.1995.tb00683.x.

Larsen, E., Longva, O., & Follestad, B. A. (1991). Formation of De Geer moraines and implications for deglaciation dynamics. *Journal of Quaternary Science*, *6*, 263–77. doi:10.1002/jqs.3390060402.

Long, A. J., Strzelecki, M. C., Lloyd, J. M., & Bryant, C. L. (2012). Dating High Arctic Holocene relative sea level changes using juvenile articulated marine shells in raised beaches. *Quaternary Science Reviews*, *48*, 61–6. doi:10.1016/j.quascirev.2012.06.009.

Lønne, I. (1997). Facies characteristics of a proglacial turbiditic sandlobe at Svalbard. *Sedimentary Geology*, *109*, 13–35. doi:10.1016/S0037-0738(96)00036-X.

Lovell, H., Fleming, E. J., Benn, D. I., Hubbard, B., Lukas, S., Rea, B. R., Noormets, R., & Flink, A. E. (2015). Debris entrainment and landform genesis during tidewater glacier surges. *Journal of Geophysical Research: Earth Surface*, *120*, 1574–95. doi:10.1002/2015JF003509.

Lundqvist, J. (1981). Moraine morphology. Terminological remarks and regional aspects. *Geografiska Annaler. Series A. Physical Geography*, (pp. 127–38). doi:10.2307/520824.

Lundqvist, J. (2000). Palaeoseismicity and De Geer Moraines. *Quaternary International*, *68*, 175–86. doi:10.1016/S1040-6182(00)00042-2.

Mackiewicz, N., Powell, R., Carlson, P., & Molnia, B. (1984). Interlaminated ice-proximal glacimarine sediments in Muir Inlet, Alaska. *Marine Geology*, *57*, 113–47. doi:10.1016/0025-3227(84)90197-X.

Mangerud, J., Bolstad, M., Elgersma, A., Helliksen, D., Landvik, J. Y., Lønne, I., Lycke, A. K., Salvigsen, O., Sandahl, T., & Svendsen, J. I. (1992). The last glacial maximum on Spitsbergen, Svalbard. *Quaternary Research*, *38*, 1–31. doi:10.1016/0033-5894(92)90027-G.

Mulder, T., & Alexander, J. (2001). The physical character of subaqueous sedimentary density flows and their deposits. *Sedimentology*, *48*, 269–99. doi:10.1046/j.1365-3091.2001.00360.x.

Noormets, R., Kirchner, N., & Flink, A. E. (2016a). Submarine medial moraines in Hambergbukta, southeastern Spitsbergen. In J. A. Dowdeswell, M. Canals, M. Jakobsson, B. J. Todd, E. K. Dowdeswell, & K. A. Hogan (Eds.), *Atlas of submarine glacial landforms* number 46 in Geological Society Memoir (pp. 61–2). The Geological Society London. doi:10.1144/M46.122.

Noormets, R., Kirchner, N., Flink, A. E., & Dowdeswell, J. A. (2016b). Possible iceberg-produced submarine terraces in Hambergbukta, Spitsbergen. In J. A. Dowdeswell, M. Canals, M. Jakobsson, B. J. Todd, E. K. Dowdeswell, & K. A. Hogan (Eds.), *Atlas of submarine glacial landforms* number 46 in Geological Society Memoir (pp. 101–2). The Geological Society London. doi:10.1144/M46.121.

Ó Cofaigh, C. (1998). Geomorphic and sedimentary signatures of early Holocene deglaciation in High Arctic fiords, Ellesmere Island, Canada: implications for deglacial ice dynamics and thermal regime. *Canadian Journal of Earth Sciences*, *35*, 437–52. doi:10.1139/e97-116.

Ó Cofaigh, C., & Dowdeswell, J. (2001). Laminated sediments in glacimarine environments: diagnostic criteria for their interpretation. *Quaternary Science Reviews*, *20*, 1411–36. doi:10.1016/S0277-3791(00)00177-3.

Ó Cofaigh, C., Dowdeswell, J., Allen, C., Hiemstra, J., Pudsey, C., Evans, J., & Evans, D. (2005). Flow dynamics and till genesis associated with a marine-based Antarctic paleo-ice stream. *Quaternary Science Reviews*, *24*, 709–40. doi:10.1016/j.quascirev.2004.10.006.

Ó Cofaigh, C., Lemmen, D., Evans, D., & Bednarski, J. (1999). Glacial landform–sediment assemblages in the Canadian High Arctic and their implications for late Quaternary glaciation. *Annals of Glaciology*, *28*, 195–201. doi:10.3189/172756499781821760.

Ottesen, D., & Dowdeswell, J. (2006). Assemblages of submarine landforms produced by tidewater glaciers in Svalbard. *Journal of Geophysical Research*, *111*, F01016. doi:10.1029/2005JF000330.

Ottesen, D., Dowdeswell, J., Benn, D., Kristensen, L., Christiansen, H., Christensen, O., & Vorren, T. (2008). Submarine landforms characteristic of glacier surges in two Spitsbergen fjords. *Quaternary Science Reviews*, *27(15)*, 1583–99. doi:10.1016/j.quascirev.2008.05.007.

Ottesen, D., Dowdeswell, J., Landvik, J., & Mienert, J. (2007). Dynamics of the Late-Weichselian ice sheet on Svalbard inferred from high-resolution sea-floor morphology. *Boreas*, *36*, 286–306. doi:10.1111/j.1502-3885.2007.tb01251.x.

Ottesen, D., Dowdeswell, J., & Rise, L. (2005). Submarine landforms and the reconstruction of fast-flowing ice streams within a large Quaternary ice sheet: the 2500-km-long Norwegian-Svalbard margin (57°– 80°N). *Geological Society of America Bulletin*, *117*, 1033–50. doi:10.1130/B25577.1.

Patton, H., Andreassen, K., Bjarnadóttir, L. R., Dowdeswell, J. A., Winsborrow, M., Noormets, R., Polyak, L., Auriac, A., & Hubbard, A. (2015). Geophysical constraints on the dynamics and retreat of the Barents Sea ice sheet as a paleobenchmark for models of marine ice sheet deglaciation. *Reviews of Geophysics*, *53*, 1051–98. doi:10.1002/2015RG000495.

Pfirman, S. L., Bauch, D., & Gammelsrød, T. (1994). The northern Barents Sea: water mass distribution and modification. *The polar oceans and their role in shaping the global environment*, (pp. 77–94). doi:10.1029/GM085p0077.

Plassen, L., Vorren, T., & Forwick, M. (2004). Integrated acoustic and coring investigations of glacigenic deposits in Spitsbergen fjords. *Polar Research*, *23(1)*, 89–110. doi:10.1111/j.1751-8369.2004.tb00132.x.

Powell, R., & Domack, E. (1995). Modern glaciomarine environments. *Glacial environments*, *1*, 445–86.

Prior, D. B., Bornhold, B., & Johns, M. (1984). Depositional characteristics of a submarine debris flow. *The Journal of Geology*, (pp. 707–27). URL: `http://www.jstor.org/stable/30070502`.

Rasmussen, T., Forwick, M., & Mackensen, A. (2012). Reconstruction of inflow of Atlantic Water to Isfjorden, Svalbard during the Holocene: Correlation to climate and seasonality. *Marine Micropaleontology*, *94-95*, 80–90. doi:10.1016/j.marmicro.2013.03.011.

Roy, S., Hovland, M., Noormets, R., & Olaussen, S. (2015). Seepage in Isfjorden

and its tributary fjords, West Spitsbergen. *Marine Geology*, *363*, 146–59. doi:10.1144/GSL.SP.1993.070.01.06.

Roy, S., Senger, K., Braathen, A., Noormets, R., Hovland, M., & Olaussen, S. (2014). Fluid migration pathways to seafloor seepage in inner Isfjorden and Adventfjorden, Svalbard. *Norwegian Journal of Geology*, *94*, 99–119. URL: `http://hdl.handle.net/1956/10661`.

Seramur, K. C., Powell, R. D., & Carlson, P. R. (1997). Evaluation of conditions along the grounding line of temperate marine glaciers: an example from Muir Inlet, Glacier Bay, Alaska. *Marine Geology*, *140*, 307–27. doi:10.1016/S0025-3227(97)00026-1.

Sexton, D. J., Dowdeswell, J. A., Solheim, A., & Elverhøi, A. (1992). Seismic architecture and sedimentation in northwest Spitsbergen fjords. *Marine Geology*, *103*, 53–68. doi:10.1016/0025-3227(92)90008-6.

Ślubowska, M. A., Koç, N., Rasmussen, T. L., & Klitgaard-Kristensen, D. (2005). Changes in the flow of Atlantic water into the Arctic Ocean since the last deglaciation: evidence from the northern Svalbard continental margin, 80° N. *Paleoceanography*, *20*. doi:10.1029/2005PA001141.

Ślubowska-Woldengen, M., Rasmussen, T., Koç, N., Klitgaard-Kristensen, D., Nilsen, F., & Solheim, A. (2007). Advection of Atlantic Water to the western and northern Svalbard shelf since 17,500 cal yr BP. *Quaternary Science Reviews*, *26*, 463–78. doi:10.1016/j.quascirev.2006.09.009.

Smith, A. M. (1997). Basal conditions on Rutford ice stream, West Antarctica, from seismic observations. *Journal of Geophysical Research: Solid Earth*, *102*, 543–52. doi:10.1029/96JB02933.

Solheim, A. (1991). The depositional environment of surging sub-polar tidewater glaciers. *Norsk Polarinstitutt Skrifter*, *194*, 1–97.

Solheim, A., & Pfirman, S. (1985). Sea-floor morphology outside a grounded, surging glacier; Bråsvellbreen, Svalbard. *Marine Geology*, *65*, 127–43. doi:10.1016/0025-3227(85)90050-7.

Spagnolo, M., Clark, C., Hughes, A., Dunlop, P., & Stokes, C. (2010). The planar shape of drumlins. *Sedimentary Geology*, *232*, 119–29. doi:10.1016/j.sedgeo.2010.01.008.

Stevens, R. (1990). Proximal and distal glacimarine deposits in southwestern Sweden: contrasts in sedimentation. *Geological Society, London, Special Publications*, *53*, 307–16. doi:10.1144/GSL.SP.1990.053.01.17.

Stewart, F., & Stoker, M. (1990). Problems Associated with Seismic Facies Analysis of Diamicton-Dominated, Shelf Glacigenic Sequences. *Geo-Marine Letters*, *10*, 151–6. doi:10.1007/BF02085930.

Stokes, C., & Clark, C. (2002). Are long subglacial bedforms indicative of fast ice flow? *Boreas*, *31(3)*, 239–49. doi:10.1111/j.1502-3885.2002.tb01070.x.

Stokes, C. R., Tarasov, L., Blomdin, R., Cronin, T. M., Fisher, T. G., Gyllencreutz, R., Hättestrand, C., Heyman, J., Hindmarsh, R. C., Hughes, A. L., Jakobsson, M., Kirchner, N., Livingstone, S., Margold, M., Murton, J. B., Noormets, R., Peltier, W. R., Peteet, D. M., Piper, D. J. W., Preussner, F., Renssen, H., Roberts, D. H., Roche, D. R., SaintAnge, F., Stroeven, A. P., & Teller, J. T. (2015). On the reconstruction of palaeo-ice sheets: recent advances and future challenges. *Quaternary Science Reviews*, *125*, 15–49. doi:10.1016/j.quascirev.2015.07.016.

Streuff, K., Forwick, M., Szczuciński, W., Andreassen, K., & Ó Cofaigh, C.

(2015). Landform assemblages in inner Kongsfjorden, Svalbard: evidence of recent glacial (surge) activity. *Arktos*, *1*. doi:10.1007/s41063-015-0003-y.

Strömberg, B. (1965). Mappings and geochronological investigations in some moraine areas of south-central Sweden. *Geografiska Annaler. Series A, Physical Geography*, *47*, 73–82. doi:10.2307/520956.

Svendsen, H., Beszczynska-Møller, A., Hagen, J., Lefauconnier, B., Tverberg, V., Gerland, S., Ørbæk, J. B., Bischof, K., Papucci, C., Zajaczkowski, M., Azzolini, R., Bruland, O., Wiencke, C., Winther, J.-G., & Dallmann, W. (2002). The physical environment of Kongsfjorden-Krossfjorden, an Arctic fjord system in Svalbard. *Polar Research*, *21(1)*, 133–66. doi:10.1111/j.1751-8369.2002.tb00072.x.

Svendsen, J. I., Gataullin, V., Mangerud, J., & Polyak, L. (2004). The glacial history of the Barents and Kara Sea region. *Developments in Quaternary Sciences*, *2*, 369–78. doi:10.1016/S1571-0866(04)80086-1.

Syvitski, J., Andrews, J., & Dowdeswell, J. (1996). Sediment deposition in an iceberg-dominated glacimarine environment, East Greenland: basin fill implications. *Global and Planetary Change*, *12*, 251–70. doi:10.1016/0921-8181(95)00023-2.

Syvitski, J., & Murray, J. (1981). Particle interaction in fjord-suspended sediment. *Marine Geology*, *39*, 215–42. doi:10.1016/0025-3227(81)90073-6.

Syvitski, J. P. (1989). On the deposition of sediment within glacier-influenced fjords: oceanographic controls. *Marine Geology*, *85*, 301–29. doi:10.1016/0025-3227(89)90158-8.

Szczuciński, W., & Zajaczkowski, M. (2012). Factors controlling downward fluxes of particulate matter in glacier-contact and non-glacier contact set-

tings in a subpolar fjord (Billefjorden, Svalbard). *International Association of Sedimentology, Special Publication*, *44*, 369–86.

Szczuciński, W., Zajaczkowski, M., & Scholten, J. (2009). Sediment accumulation rates in subpolar fjords – impact of post-Little Ice Age glacier retreat, Billefjorden, Svalbard. *Estuarine, Coastal and Shelf Science*, *85*, 345–56. doi:10.1016/0025-3227(89)90158-8.

Tulaczyk, S., Scherer, R., & Clark, C. (2001). A ploughing model for the origin of weak tills beneath ice streams: a qualitative treatment. *Quaternary Internationals*, *86*, 59–70. doi:10.1016/S1040-6182(01)00050-7.

Van der Veen, C. J. (1999). Crevasses on glaciers 1. *Polar Geography*, *23*, 213–45. doi:10.1080/10889379909377677.

Woodworth-Lynas, C., & Guigné, J. (1990). Iceberg scours in the geological record: examples from glacial Lake Agassiz. *Geological Society, London, Special Publications*, *53*, 217–33. doi:10.1144/GSL.SP.1990.053.01.12.

Zilliacus, H. (1989). Genesis of De Geer moraines in Finland. *Sedimentary geology*, *62*, 309–17. doi:10.1016/0037-0738(89)90121-8.

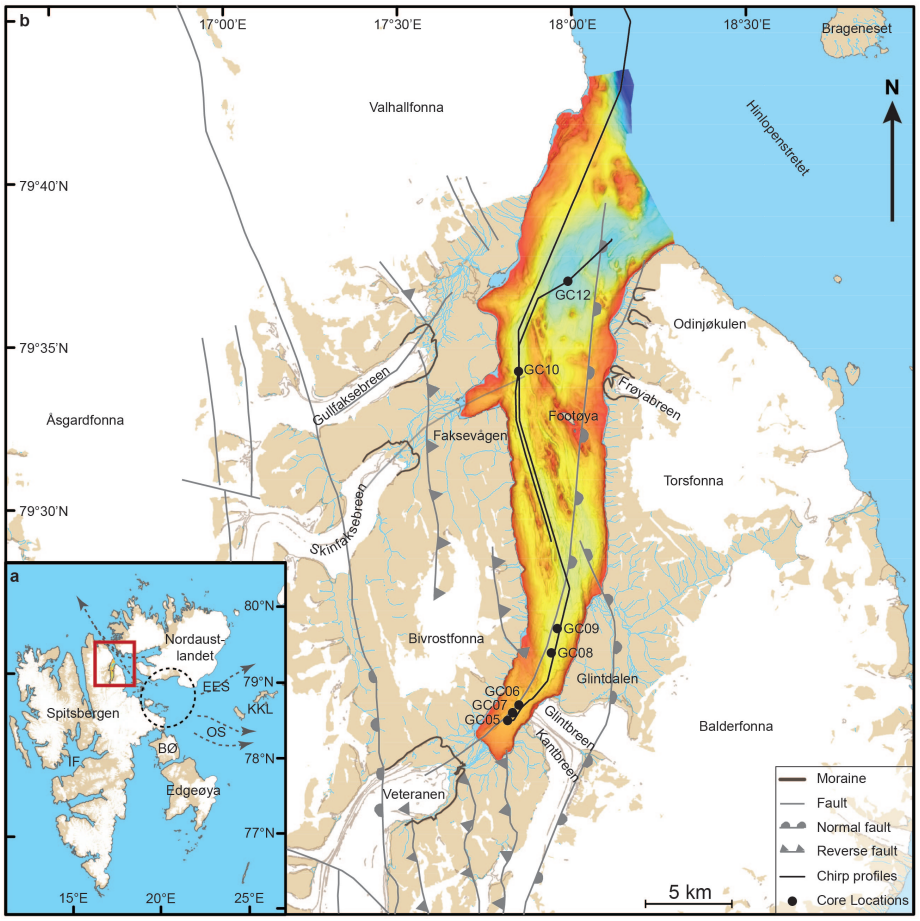

Figure 1: a) Overview map of Svalbard with red rectangle indicating the area presented in b. EES = Erik Eriksenstretet, OS = Olgastretet, KKL = Kong Karls Land, BØ = Barentsøya, IF = Isfjorden. Black circle and grey arrows indicate position of the suggested ice dome and ice flow directions, respectively, during the Late Weichselian (Landvik et al., 1998; Dowdeswell et al., 2010). b) Study area with swath bathymetry, chirp lines (black lines) and core locations (black dots) available for this study. Basemap data are courtesy of the Norwegian Polar Institute (geodata.npolar.no). Light brown lines on glaciers represent moraines.

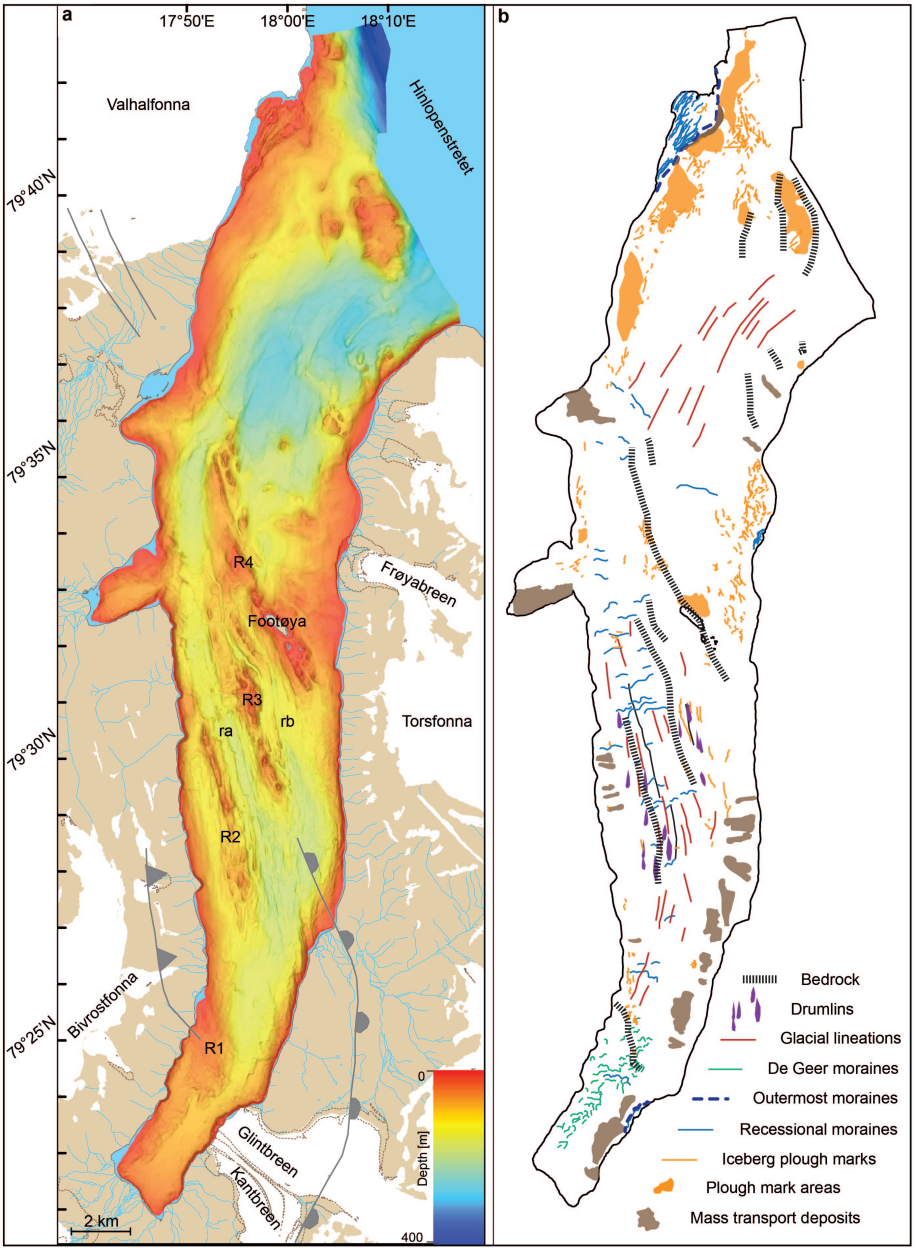

Figure 2: a) Bathymetry of the study area with faults (grey lines; information from geodata.npolar.no) and larger ridges (R1–R4, ra, rb) indicated. See Figure 1 for full legend. b) Morphological map of the landforms observed in Lomfjorden.

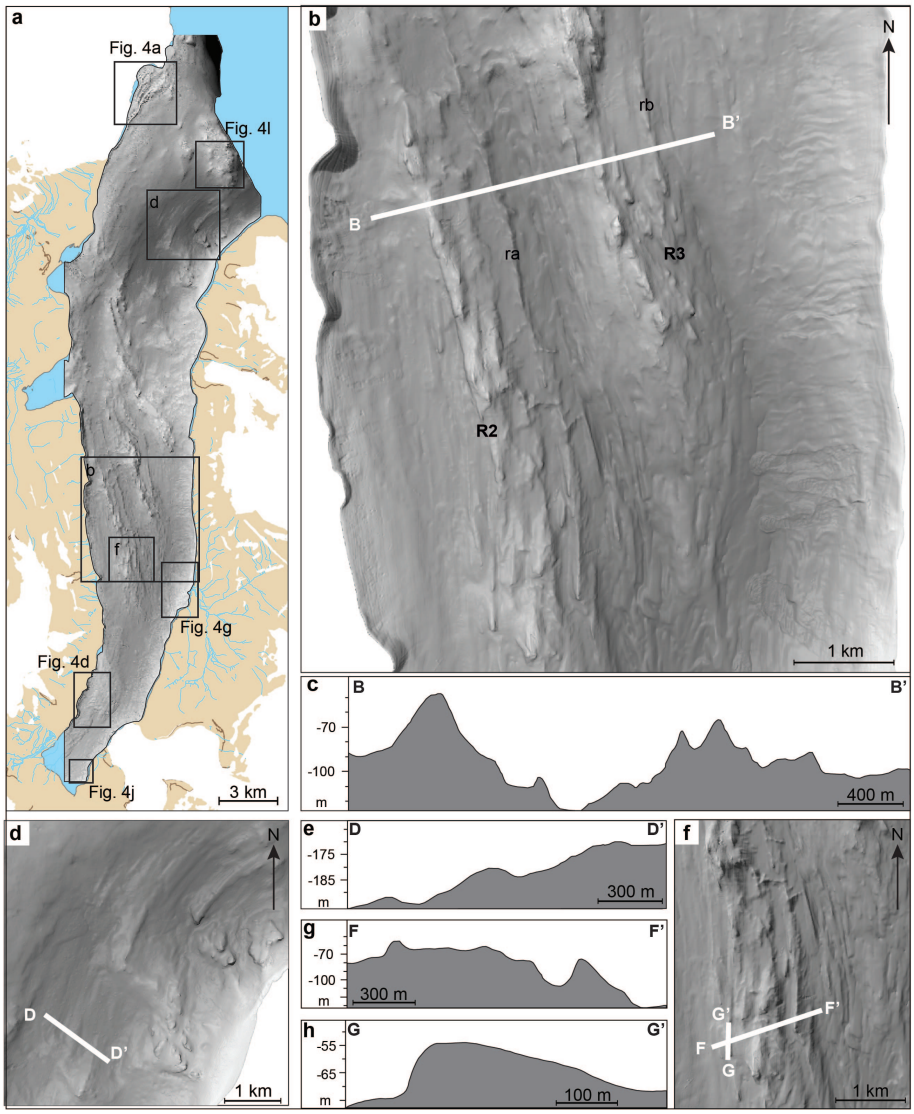

Figure 3: a) Overview of the bathymetric data and the locations for subfigures of this figure and Figure 4. b) Example of the bedrock ridges in Lomfjorden with cross-sectional profile B-B' shown in c). d) Glacial lineations in the outer fjord with cross-sectional profile D-D' shown in e). f) Drumlins in the inner fjord with two cross-sectional profiles F-F' and G-G' displayed in g) and h), respectively.

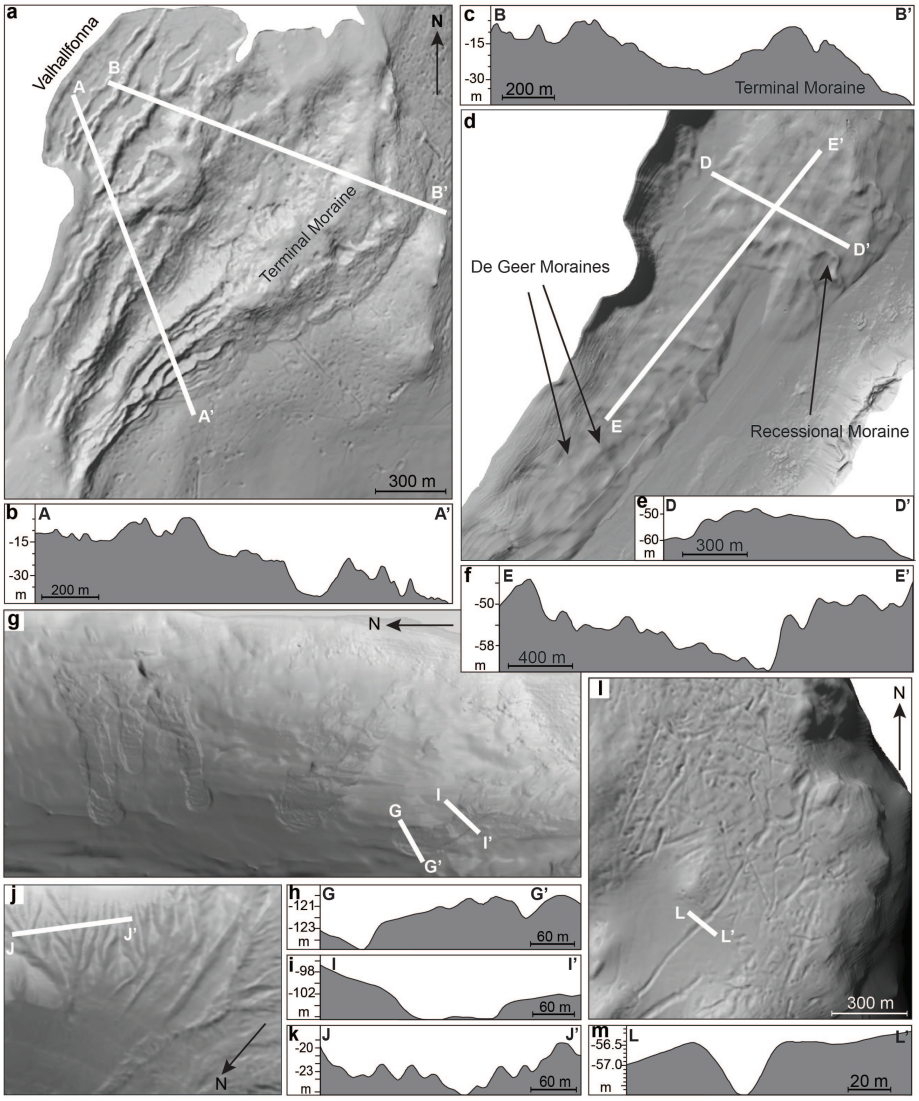

Figure 4: a) Moraines in front of Valhallfonna with cross-sectional profile A–A' displayed in b), and profile B–B' shown in c). d) Example of De Geer moraines in the inner fjord with cross-sectional profiles D–D' and E–E' shown in e) and f). g) Example of mass-transport deposits in Lomfjorden, with cross-sectional profile G-G' (deposit) in h) and I-I' (Type-A trough) in i). j) Example of submarine channel (Type-B trough) along the fjord walls with cross-sectional profile J-J' shown in k). l) Example of iceberg ploughmarks in the outer fjord with cross-sectional profile L-L' displayed in m).

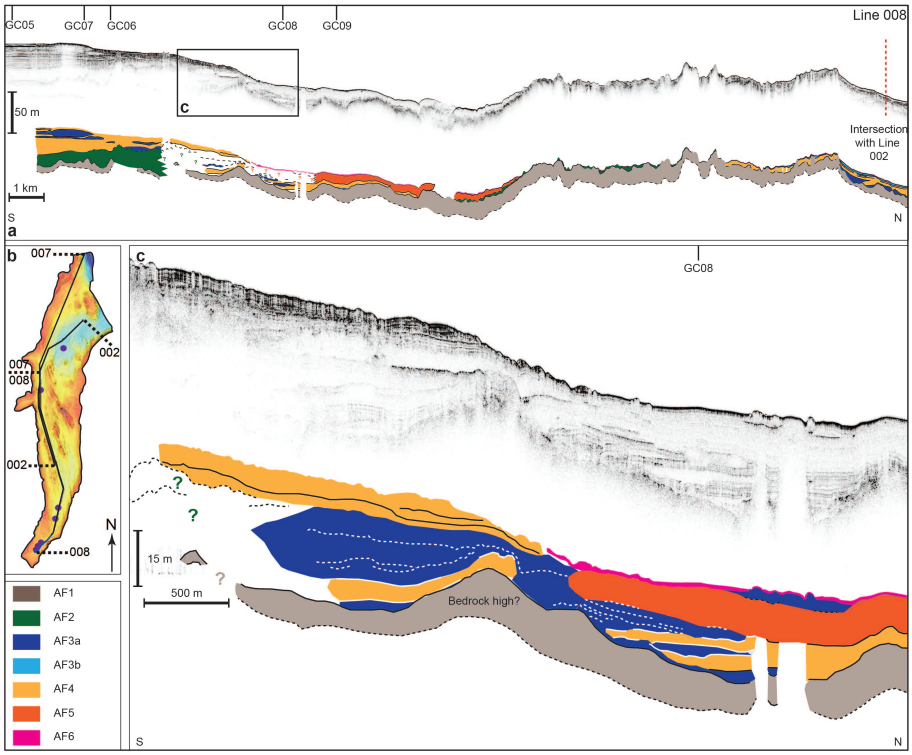

Figure 5: a) Chirp line 008 from south to north with the interpretation of acoustic facies underneath. Locations of gravity cores are indicated. The black rectangle shows the extent of c). Conversion between m and ms was based on an assumed p-wave velocity of 1500 m s^{-1}. b) Location of the chirp lines (002, 007, 008) and core sites with respect to the bathymetric data. c) Detail figure of Line 008 and the associated acoustic facies interpretation.

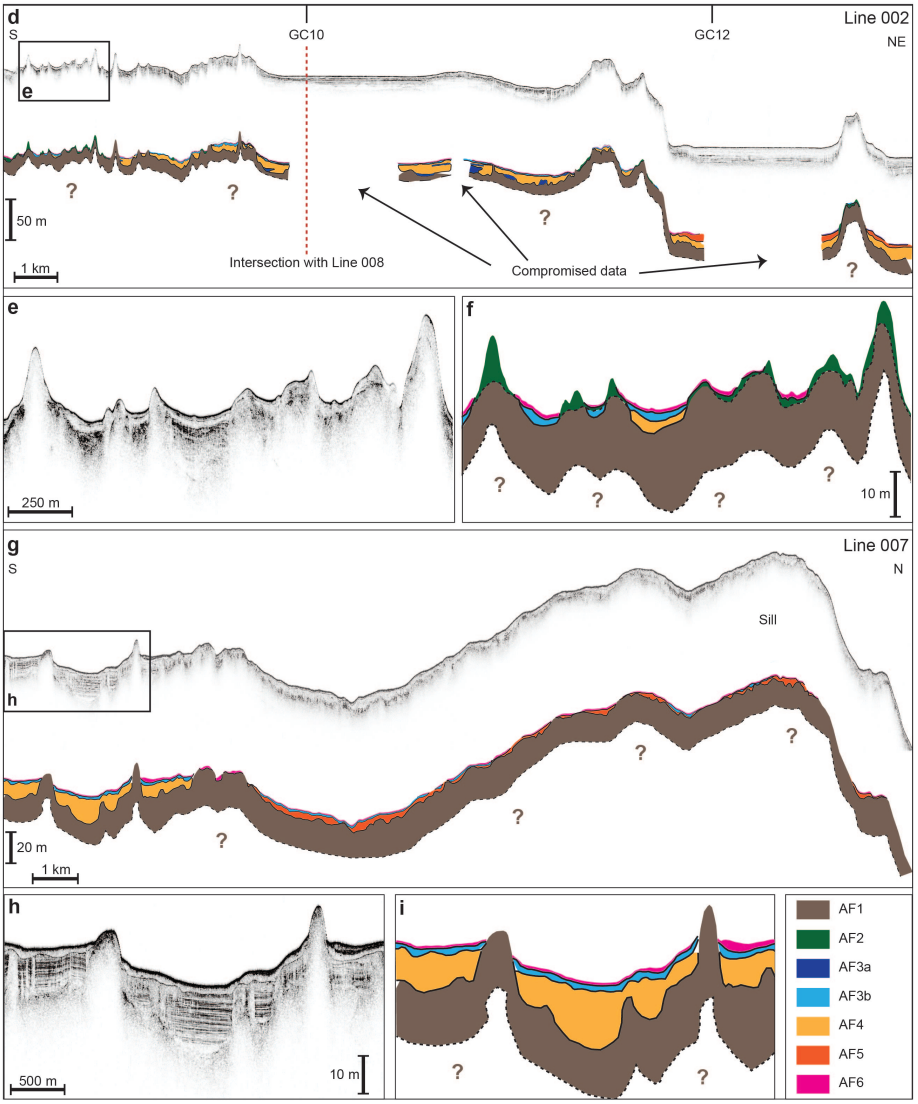

Figure 5 (cont.): d) Line 002 through the outer fjord with the according interpretation of the acoustic facies. The black rectangle indicates the extent of e), detail figure of Line 002 with the acoustic facies interpretation shown in f). g) Line 007 through the outer fjord and associated facies interpretation. The black rectangle shows the extent of h), a detail figure of Line 007 with its acoustic facies interpretation in i).

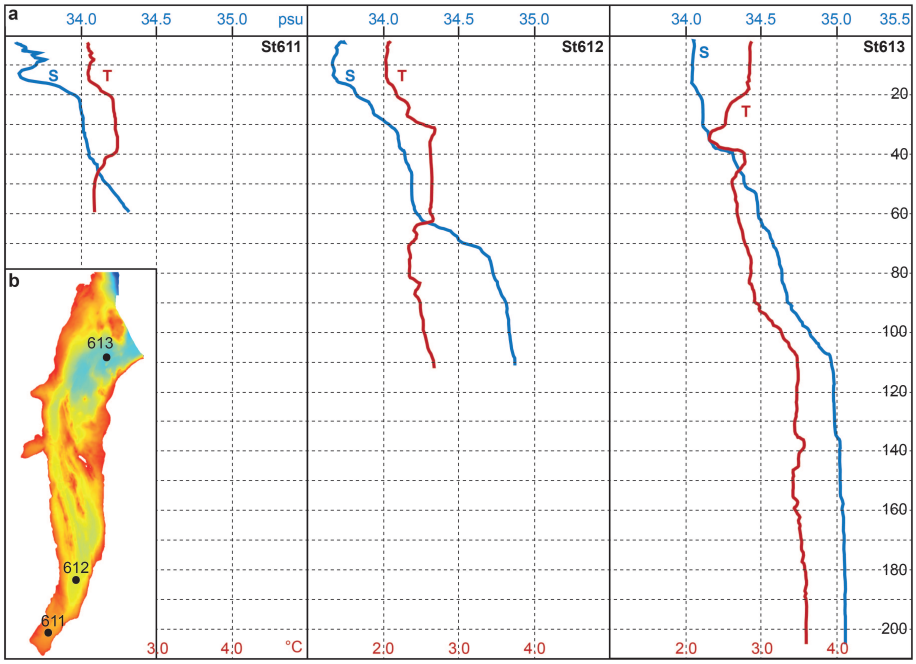

Figure 6: a) Conductivity-Temperature-Depth data from the water column at three different sites in Lomfjorden. Y-axis shows water depth in metres, whereas the x-axes show S = salinity in psu and T= temperature in °C. b) Location of the three CTD sites.

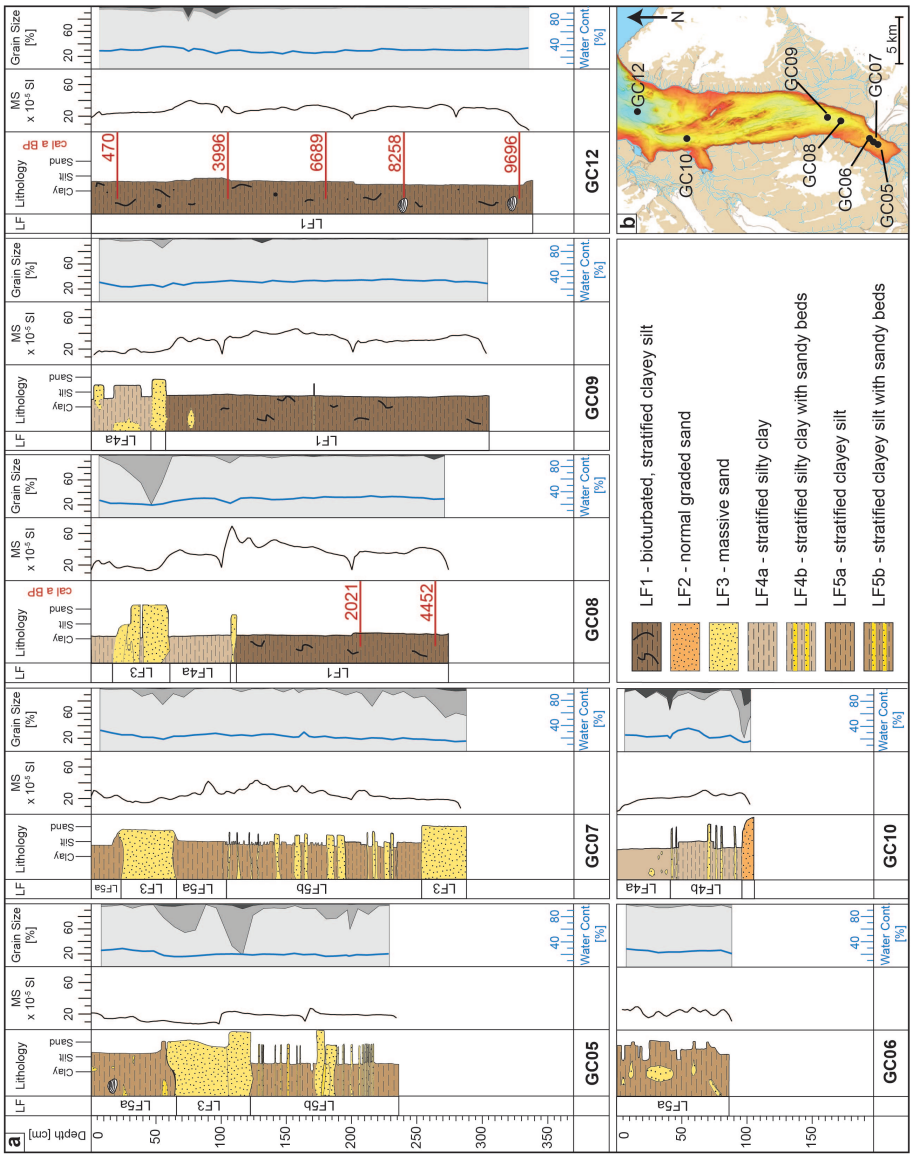

Figure 7: a) Lithofacies logs of all gravity cores with magnetic susceptibility (MS), water content and grain size distribution in weight percent. For the grain size plots, light grey areas = sediment fraction <63 μm, medium grey areas = sediment fraction 63–250 μm, and dark grey areas = sediment fraction >250 μm, the latter classified as IRD. b) Overview of the core locations in Lomfjorden.

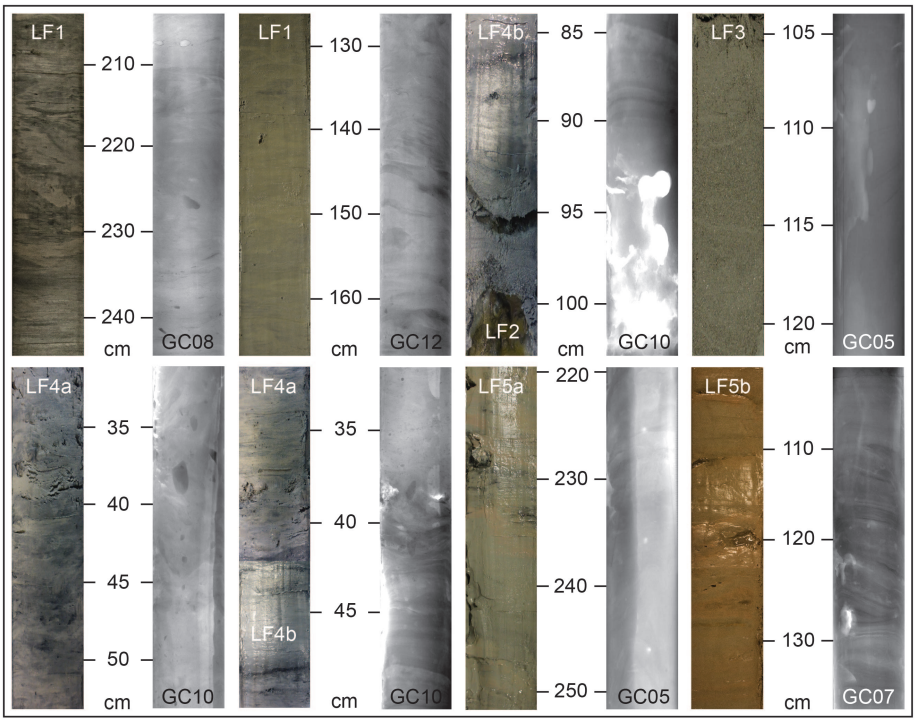

Figure 8: Examples of core photos and x-radiographs of each of the lithofacies in Lomfjorden. On the x-radiographs darker areas represent denser material.

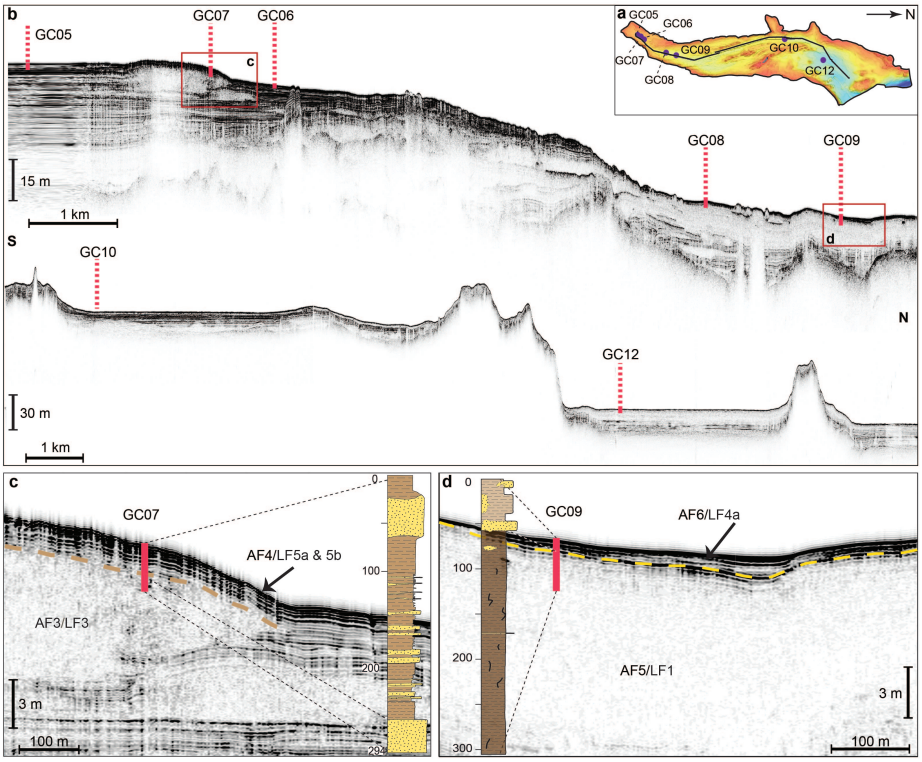

Figure 9: a) Overview of bathymetry, chirp lines 008 (left) and 002 (right) and sediment cores from Lomfjorden. Conversion between m and ms was based on an assumed p-wave velocity of 1500 m s^{-1}. b) Chirp lines 008 (top) and 002 (bottom) with approximate penetration depths of the sediment cores. c) Sediment core GC07 and its lithological units with respect to the acoustic facies. d) Sediment core GC09 and its lithological units with respect to the acoustic facies.

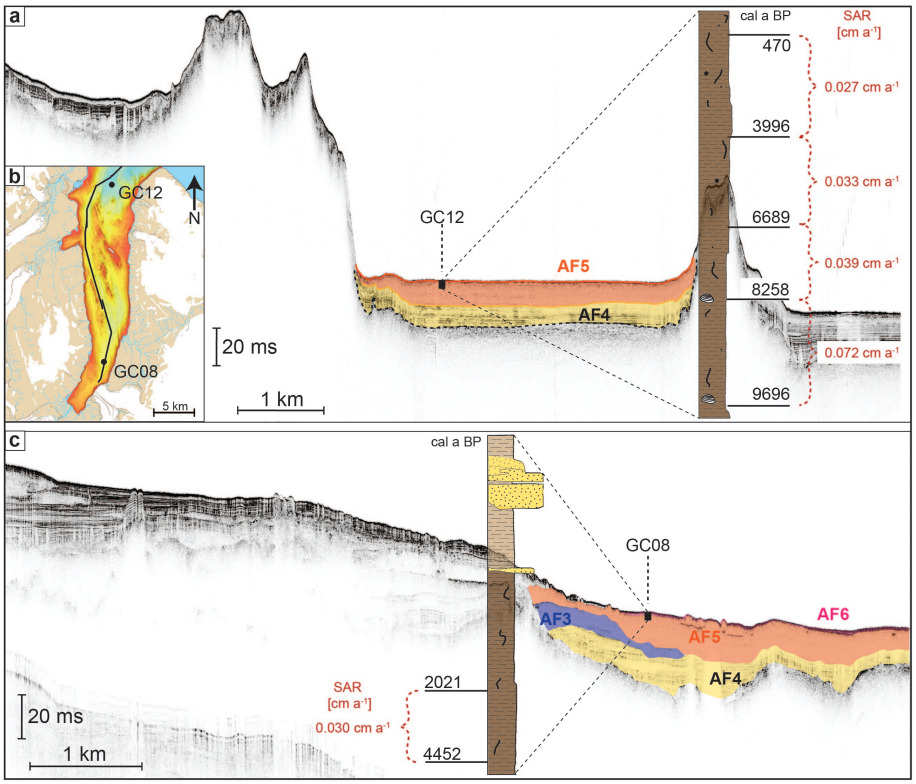

Figure 10: Radiocarbon dates and sediment accumulation rates. a) Chirp line 002 from the outer fjord showing the approximate location of GC12 with the core log, radiocarbon dates and calculated sediment accumulation rates. Note that the chirp line does not cover the core site of GC12 and the sedimentary environment for this core can thus only be inferred. Conversion between m and ms was based on an assumed p-wave velocity of 1500 m s^{-1}. b) Overview of the location of the chirp lines in a) and c) and the core sites of GC08 and GC12. c) Chirp line 008 through the inner and central fjord and the sedimentary environment of GC08. The core log with radiocarbon dates and calculated sediment accumulation rates is also shown.

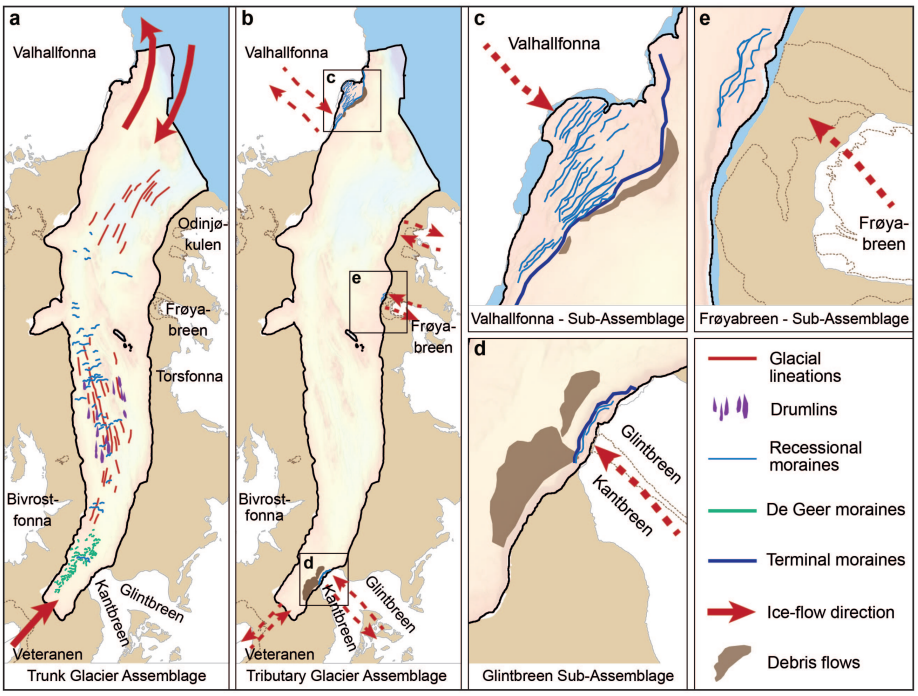

Figure 11: Landform assemblages distinguished in Lomfjorden. a) Trunk Glacier Assemblage related to trunk ice streaming through the fjord; b) Tributary Glacier Assemblage with c), d), e) detailed maps of individual assemblages in front of the three tributaries Valhallfonna (c), Glintbreen/Kantbreen (d), and Frøyabreen (e). The Tributary Assemblages could have formed during ice advance or retreat (dashed red arrows).